International Journal of Bifurcation and Chaos, Vol. 18, No. 10 (2008) 3029–3052

GENERALIZED HÉNON MAPS AND SMALE HORSESHOES OF NEW TYPES

SERGEY GONCHENKO*, MING-CHIA LI† and MIKHAIL MALKIN‡
*Research Institute of Applied Mathematics and Cybernetics,
Nizhny Novgorod State University,
Nizhny Novgorod, Russia
gosv100@uic.nnov.ru

†Department of Applied Mathematics,
National Chiao Tung University,
Hsinchu 300, Taiwan
mcli@math.nctu.edu.tw

‡Department of Mathematics and Mechanics,
Nizhny Novgorod State University,
Nizhny Novgorod, Russia
malkin@unn.ru

Received September 19, 2007; Revised November 21, 2007

We study hyperbolic dynamics and bifurcations for generalized Hénon maps in the form $\overline{x} = y, \overline{y} = \gamma y(1-y) - bx + \alpha xy$ (with b, α small and $\gamma > 4$). Hyperbolic horseshoes with alternating orientation, called half-orientable horseshoes, are proved to represent the nonwandering set of the maps in certain parameter regions. We show that there are infinitely many classes of such horseshoes with respect to the local topological conjugacy. We also study transitions from the usual orientable and nonorientable horseshoes to half-orientable ones (and vice versa) as parameters vary.

Keywords: Hénon map; Smale horseshoe; half-orientable horseshoe; hyperbolic dynamics; nonwandering set; singular bifurcation.

1. Introduction

The classical Hénon map

$$\overline{x} = y, \quad \overline{y} = 1 - bx + ay^2, \tag{1}$$

where $(x, y) \in \mathbb{R}^2$ and a, b are real parameters, was introduced in [Hénon, 1976] as a very simple planar map demonstrating chaotic dynamics. Map (1) can be rewritten in an equivalent form (if $a \neq 0$) as follows

$$\overline{x} = y, \quad \overline{y} = M - bx - y^2, \tag{2}$$

which is called *the standard form* of the Hénon map.

Since 1976, the time of publication [Hénon, 1976], the Hénon map has quickly become one of the most popular chaotic model maps, and many papers have been devoted to the study of its dynamics. The main reason for such an interest is due to the fact that the Hénon map can be considered as the simplest nonlinear mathematical model having important properties of multidimensional chaotic systems. We also remark that the Hénon map cannot be regarded as a purely artificial one. It may appear in applied dynamics: in particular, systems with homoclinic tangencies can be considered as a natural source for Hénon-like maps (see [Gavrilov & Shinikov, 1972, 1973; Tedeschini-Lalli & Yorke, 1986; Gonchenko *et al.*, 1993, 1996, 2005a, 2005b]).

However, the Hénon map itself has, definitely, rather restricted applications in the bifurcation theory because this map can be regarded as an *infinitely degenerate* one with respect to the following two aspects:

(i) bifurcations of periodic points with multipliers $e^{\pm i\varphi}$;
(ii) transitions from orientable maps (for $b > 0$) to nonorientable ones (for $b < 0$).

Indeed, in the Hénon family, no closed invariant curves appear via Andronov–Hopf bifurcations and, moreover, no closed invariant curves exist, except for the KAM-curves with $b = \pm 1$. As for the second aspect, note that at the critical moment, $b = 0$, the Hénon map becomes one-dimensional: namely, all periodic points have zero multiplier and, moreover, their unstable manifolds coincide totally (which implies, certainly, the infinitely degenerate situation in the two-dimensional setting).

Thus, it is reasonable to extend the Hénon family to consider the mentioned problems for maps close to the Hénon map, and there appears another problem: what is a "natural" extension that one should study? Fortunately, we can use the homoclinic approach, which leads to *Generalized Hénon Maps* (GHM, for abbreviation). There are two main forms for GHMs (see [Gonchenko & Gonchenko, 2000, 2004; Gonchenko *et al.*, 2005a, 2005b]. The first one is given by quadratic extension as follows:

$$\bar{x} = y, \quad \bar{y} = M - b_1 x - y^2 + \nu_1 xy, \tag{3}$$

and the second one is given by the cubic extension:

$$\bar{x} = y, \quad \bar{y} = M - b_1 x - y^2 + \nu_1 xy + \nu_2 y^3. \tag{4}$$

where, in both formulas (3) and (4), ν_1 and ν_2 are small enough.

It was shown in [Gonchenko & Gonchenko, 2000, 2004] that GHMs demonstrate nondegenerate Andronov–Hopf bifurcations provided $\nu_1 \neq 0$. The case when ν_1, ν_2 are small and b_1 is positive was considered in [Gonchenko & Gonchenko, 2000, 2004], see also [Shilnikov *et al.*, 2001]. In [Gonchenko *et al.*, 2005a, 2005b], bifurcations were studied for GHMs with arbitrary ν_1, ν_2 and b_1. Thus, one may say that the mentioned aspect (i) concerning degeneracy of the Hénon map, is resolved successfully whenever one considers GHMs instead.

Aspect (ii) is concerned in the present paper. Especially we will study hyperbolic dynamics of GHMs. Our main attention will be paid to map (3) that can be rewritten (for those parameter domains where fixed points exist) in the following "parabola-like form"

$$\bar{x} = y, \quad \bar{y} = \gamma y(1 - y) - bx + \alpha xy, \tag{5}$$

where $b = b_1 + \nu_1\gamma/2$, $\alpha = \nu_1\gamma/2$ and

$$\gamma = \frac{b_1 + 1 + \sqrt{(b_1 + 1)^2 + 4M(1 + \nu_1)}}{1 - \nu_1}.$$

We suppose that b and α are sufficiently small. We prefer the parabola-like form for GHM since it is "well suited" for the study of the nonwandering sets, which can be shown to be bounded even for large scale of parameters involved (see [Li & Malkin, 2004]). Besides, when b and α are small enough, we may use the information on the orbit structure of the (well-known) one-dimensional map $\bar{y} = \gamma y(1 - y)$ due to results on multidimensional perturbations of low-dimensional maps (see [Misiurewicz & Zgliczynski, 2001; Juang *et al.,* 2005; Li & Malkin, 2006]. Since the (standard) Hénon map can be considered as a particular case of GHMs for which $\alpha = 0$ in (5), we will usually keep in mind the form (5) with $\alpha = 0$ when speaking of the Hénon map.

It is well known that only two different types of horseshoes[1] can be observed for the Hénon map. Namely, for $b > 0$, the horseshoes are orientable, and for $b < 0$ they are nonorientable; see Fig. 1, which illustrates the geometry of such horseshoes. Here, the image of some square Q, containing the unit square $Q_0 = [0, 1]\times[0, 1]$, has a horseshoe shape but its orientation is different for the cases $b > 0$ and $b < 0$.

However, hyperbolic dynamics of GHMs is much richer, as we will show below. It turns out, that in some regions of parameters, the nonwandering (hyperbolic) set of GHM can be represented by horseshoes of new types, called *half-orientable*, though the usual orientable and nonorientable horseshoes for certain values of parameters may exist as well. The appearance of such horseshoes for GHMs (5) is caused by the fact that the Jacobian of map (5), which equals $J = b - \alpha y$, is

[1]In the literature, and in the present paper as well, the term "horseshoe" is meant sometimes as the horseshoe map, or the nonwandering (Cantor) set for this map, or just as the horseshoe shape for the first (pre)image of some square. We hope that the precise meaning would be clear from the context.

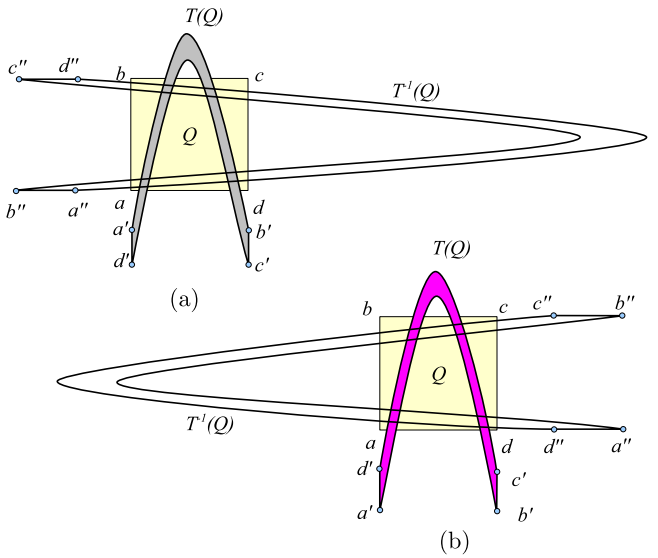

Fig. 1. Horseshoes in the standard Hénon map for small b: (a) the orientable case ($b > 0$); (b) the nonorientable case ($b < 0$). Routes $a \to b \to c \to d \to a$ and $a' \to b' \to c' \to d' \to a'$ have the same direction in case (a) and opposite direction in case (b).

not a constant in $\mathbb{R}^2$, unlike for the Hénon map. Thus, if the line $y = b/\alpha$ (where the Jacobian vanishes) intersects the square Q, then the map transforms Q into a horseshoe which has different orientations in two parts: $y > b/\alpha$ and $y < b/\alpha$. Besides, it is easily seen that the line $y = b/\alpha$ is mapped into a single point $P^* = \alpha^{-1}(b, \gamma b(1 - (b/\alpha)))$. The point P^* will be referred to as the *collapse point*. We will show that there are various types of half-orientable horseshoes depending on the position of the collapse point. Some of such horseshoes are illustrated in Fig. 2. In a sense, horseshoes (a) and (b) in Fig. 2 can be considered as an analog of the usual Smale horseshoe since the collapse point is posed outside Q. Therefore, we will call such horseshoes (i.e. ones with collapse point outside Q) the *half-orientable horseshoes of simple type*. On the other hand, it turns out that the horseshoes with the collapse point inside Q (like (c) and (d) in Fig. 2) could be much more interesting and multifarious, and we study them in the present paper.

As we said before, for the Hénon map, the moment $b = 0$ corresponds to the bifurcation when the "instant" transition from orientable to nonorientable horseshoes (or vice versa) occurs. Though GHMs may also have usual orientable and nonorientable horseshoes, the transition between horseshoes of different orientation is not as trivial as for the Hénon map. We will show below that numerous bifurcations occur while this transition takes place for GHMs. More precisely, the parameter space (α, b), for any fixed $\gamma > 4$, can be divided by bifurcation curves into (infinitely many) open regions in each of which the corresponding map (5) is hyperbolic. Every such bifurcation corresponds to the situation when infinitely many points of the horseshoe are mapped into the collapse point. Though all the horseshoes remain mutually Ω-conjugate (since any horseshoe, by definition, is conjugate to $\mathcal{B}_2$, the two-sided Bernoulli shift with two symbols), they need not be locally conjugate.[2] We describe this phenomenon by indicating those bifurcations which change the type of border periodic points (see Definition 1 below). It is known [Grines, 1975] that periods of border periodic points are the same for locally conjugate hyperbolic sets. We detect infinitely many bifurcations that lead to the appearance of border points of arbitrarily large periods, which proves the existence of *infinitely many classes* (with respect to local conjugacy) of half-orientable horseshoes.

The presented results on dynamics and bifurcations of GHMs look very natural, but surprisingly, we have found only few related results in the literature. Border periodic points of basic hyperbolic sets for diffeomorphisms on surfaces were first introduced and applied to the classification problems in [Grines, 1975]. The approach to the study of geometrical structure of horseshoes based on border points (in somewhat different terms) goes back to [Afraimovich, 1984]. Some elements of chaotic dynamics for GHMs with small b were described in [Gonchenko *et al.*, 2005a, 2005b]. On the other hand, the topic of hyperbolic and chaotic dynamics for two-dimensional noninvertible polynomial maps (endomorphisms) is very popular, and there is a vast list of relevant papers (we refer readers to books [Mira, 1987; Mira *et al.*, 1996] and references therein). Nevertheless, most of the problems in those papers and books

[2]Two maps T, T' are called Ω-*conjugate* if there exists a homeomorphism $h : \Lambda \to \Lambda'$ of their nonwandering sets Λ, Λ' such that $h \circ T(x) = T' \circ h(x)$ for all $x \in \Lambda$. The maps T and T' are said to be *locally conjugate* if for any neighborhoods U and U' of Λ and Λ' respectively, there exist smaller neighborhoods $\tilde{U} \subset U$, $\tilde{U}' \subset U'$ and a homeomorphism $\tilde{h} : \tilde{U} \to \tilde{U}'$ such that $\tilde{h}(\Lambda) = \Lambda'$ and $\tilde{h} \circ T(x) = T' \circ \tilde{h}(x)$ for all $x \in \tilde{U} \cap T^{-1}(\tilde{U})$; in this case the sets Λ, Λ' are also called *locally equivalent*.

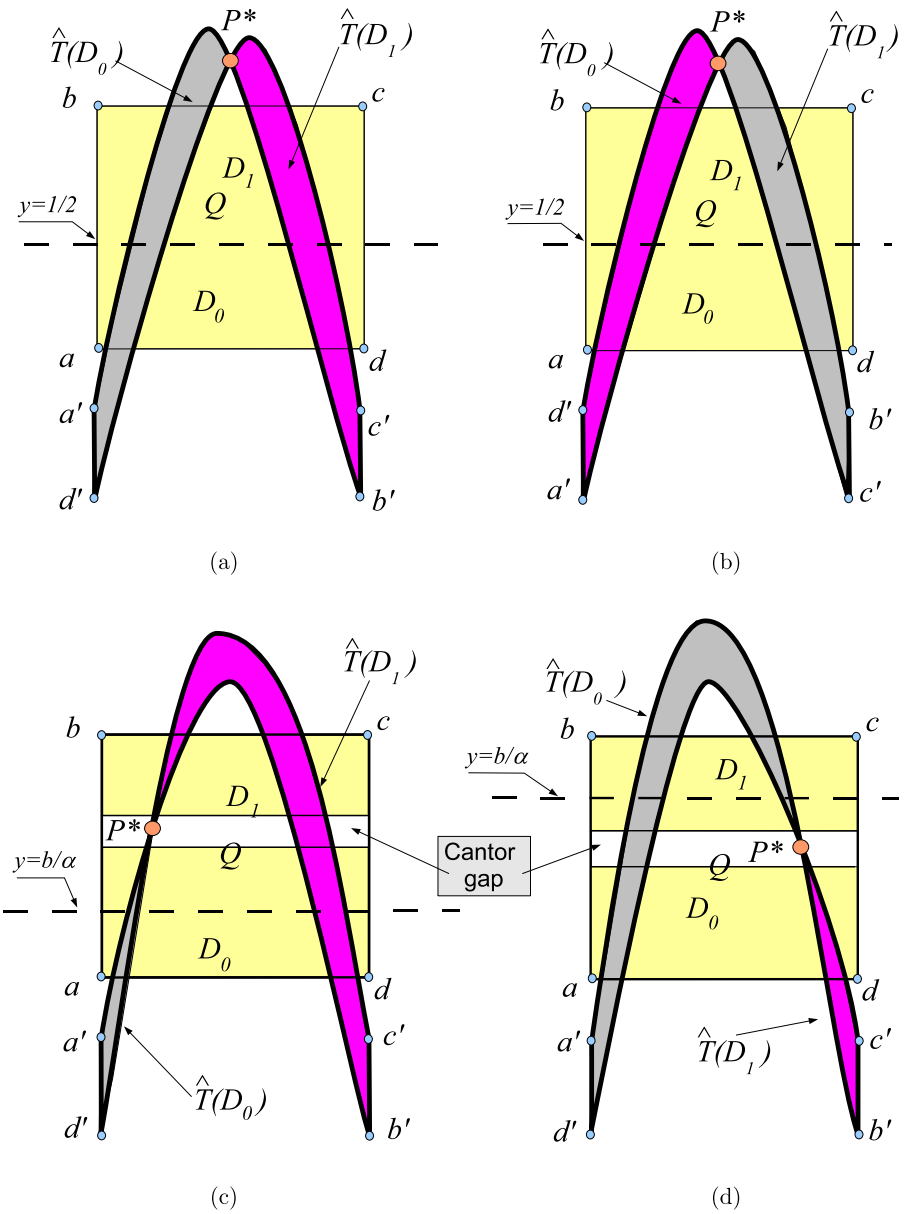

Fig. 2. Half-orientable horseshoes in GHM: (a) for $b/\alpha = 1/2$ and $b > 0$; (b) for $b/\alpha = 1/2$ and $b < 0$; (c) for $0 < b/\alpha < 1/2$ and $b > 0$; (d) for $1/2 < b/\alpha < 1$ and $b > 0$.

are devoted to maps which look different from Hénon-like maps and demonstrate another type of hyperbolic behavior: they usually have limit sets like snap-back repellers [Marotto, 1978; Gardini *et al.*, 1994]. Perhaps, this is caused by the fact that dynamics of Smale horseshoes seemed to be "too well-known", and "no news" were expected here. So this paper shows, in a sense, that bifurcations of horseshoe structures from the geometrical point of view still have interesting features. Let us summarize these features for GHMs:

(i) The bifurcations of GHM horseshoes do not lead off the class of hyperbolic systems, though there might appear singular nonwandering orbits (with zero multipliers or Lyapunov exponents equal to $-\infty$); at the bifurcation moments the map on the nonwandering set is not conjugate to the Bernoulli shift, so one has such a degenerate hyperbolicity at these moments.

(ii) The above bifurcations are "instant": just away from the bifurcation values one has (nondegenerate) Smale horseshoes again.

(iii) Though all these horseshoes are Ω-conjugate to $\mathcal{B}_2$, they could be distinguished in the following sense: the border points may have different

periods and, moreover, the periods can be arbitrarily large. As a consequence, we show that there are infinitely many types of horseshoes with respect to the local equivalence relation.

1.1. *Main results*

Our main results deal with hyperbolic dynamics of GHMs (5) for b and α sufficiently small. We assume also that $\gamma > 4$ is fixed. If $\alpha = b = 0$ we have the one-dimensional parabola map $\bar{y} = \gamma y(1-y)$, and it is well known that this map has hyperbolic dynamics for $\gamma > 4$; notice that hyperbolicity is meant here in the one-dimensional setting. When b and α become nonzero but still sufficiently small, one has hyperbolic structure (in two-dimensional setting) for nonwandering orbits, and now the nonwandering set is conjugate to the Smale horseshoe (see Sec. 4 for more details; in fact, there are bifurcation curves in the parameter space (α, β) where "degenerate" hyperbolicity takes place). However, from the geometrical viewpoint, horseshoes here may differ from the usual orientable and nonorientable horseshoes of the Hénon map. Our first result is concerned with existence of half-orientable horseshoes of simple type. For this, we consider the additional assumption $\alpha = 2b$, which guarantees that the collapse point P^* lies above the unit square and so, P^* is wandering. More precisely, the following holds. Let us denote map (5) by $\hat{T} \equiv \hat{T}(\gamma, b, \alpha)$.

Theorem 1. *Let $\gamma > 4$ be fixed and assume that α and b are sufficiently small and satisfy $\alpha = 2b$. Then there exists a square $Q_\beta = [-\beta, 1+\beta] \times [-\beta, 1+\beta]$ in the (x, y)-plane with $\beta \to +0$ as $b, \alpha \to 0$, and the following properties hold.*

1. *The nonwandering set Λ of the map $\hat{T}$ is the horseshoe, i.e. Λ is a uniformly hyperbolic closed set and $\hat{T}|_\Lambda$ is conjugate to the full shift $\mathcal{B}_2$.*
2. *The set Λ belongs to Q_β and is disjoint from some neighborhoods of the lines $x = 1/2$ and $y = 1/2$.*
3. *If $b > 0$ then the map $\hat{T}$ is orientable for $y < 1/2$ and nonorientable for $y > 1/2$. If $b < 0$, then the map $\hat{T}$ is nonorientable for $y < 1/2$ and orientable for $y > 1/2$.*

The proof of Theorem 1 is given in Secs. 3.1 and 4, however, geometrically, it is rather transparent and we can outline it now. When α, b are small enough and $\alpha = 2b$, the horseshoes look like in Fig. 2 (a) for $b > 0$ and (b) for $b < 0$. Note that the Jacobian of map (5) is equal to $J \equiv b - \alpha y$ and, therefore, J vanishes on the line $y = b/\alpha = 1/2$. The line $y = b/\alpha$ is mapped under $\hat{T}$ into the collapse point P^*. Since $\alpha = 2b$ and $\gamma > 4$, the point $P^* = (x^*, y^*)$ has coordinates $(1/2, \gamma/4)$ and is away from the square $Q_0 = [0,1] \times [0,1]$, so P^* is wandering. Take the square Q_β (from Theorem 1) with some small positive β. Then $\hat{T}$ acts on Q_β as a horseshoe map. But this map has a certain peculiarity. The line $y = 1/2$ divides the square Q_β into two rectangles D_0 (with $-\beta < y < 1/2$) and D_1 (with $1/2 < y < 1 + \beta$), and the map $\hat{T}$ has different orientations on D_0 and D_1. Namely, if $b > 0$, it is orientable on D_0 and nonorientable on D_1; and if $b < 0$, it is orientable on D_1 and nonorientable on D_0. So the cases $b > 0$ and $b < 0$ correspond to two different types of half-orientable horseshoes, see Figs. 2(a) and 2(b).

Remark 1. It is worth mentioning that half-orientable horseshoes can also be realized in geometrical models of Lorenz attractors, which can be represented, essentially, as suspensions over special discontinuous piecewise smooth maps of the two-dimensional disk (see [Afraimovich *et al.*, 1983] for more details). In Fig. 3, possible shapes for such maps are shown with different combinations of orientation on the rectangles D_1 and D_2. Thus, one may have here horseshoes of different types (orientable, nonorientable and half-orientable of simple type as well). We thank professor L. P. Shilnikov for calling our attention to this fact.

Thus, these simple considerations give us four different types of horseshoes: two of them are the usual orientable and nonorientable horseshoes and the other two represent half-orientable horseshoes. Although all these horseshoes are Ω-equivalent to each other (since the restriction of maps on them is conjugate to $\mathcal{B}_2$), they may differ with respect to the local equivalence relation, and moreover, as we will show below, there are infinitely many classes of half-orientable horseshoes of types different from those described in Theorem 1 (some horseshoes of new types are shown in Figs. 2(c) and 2(d)). Actually, they may have *border points* of different dynamical nature.

Definition 1. Let Λ be a closed invariant hyperbolic set of a transitive two-dimensional map T, and let $P \in \Lambda$. A saddle periodic point P of T is said to be s-border (resp. u-border), if any sufficiently small

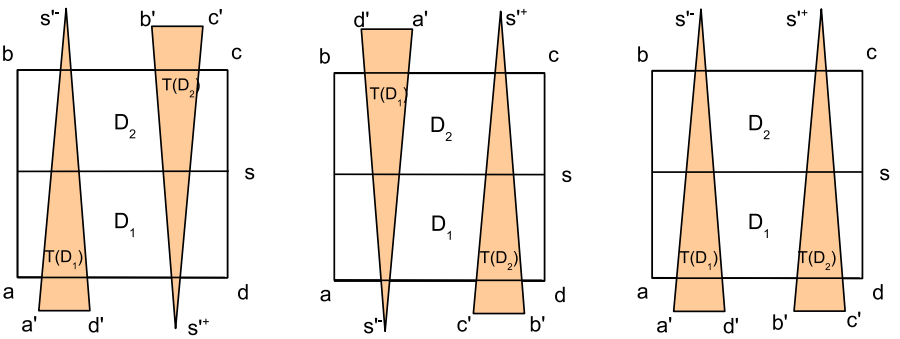

(a) (b) (c)

Fig. 3.

neighborhood of P is divided by $W^s_{\rm loc}(P)$ (resp. $W^u_{\rm loc}(P)$), the arc of the stable (resp. unstable) manifold of P, into two discs, one of which does not contain points of Λ, while the other does contain. If P is both s-border and u-border, the point P is said to be (s,u)-border.

The following Theorem 2 describes border points for orientable, nonorientable and half-orientable horseshoes of simple type as well. We will show that the set of border points has different dynamical type for each of these cases. To state Theorem 2, we need some notations. Let O_1 (resp. O_2) be the saddle fixed point of the map $\hat{T}$ with unstable eigenvalue > 1 (resp. with unstable eigenvalue < -1). Note that any horseshoe $\Lambda(\hat{T})$ contains such points. Let P_2 be a period-2 saddle cycle from Λ (recall, that in any horseshoe there is such a unique cycle).

Theorem 2. *For orientable horseshoes, the set of border points consists of a single point O_1, which is (s,u)-border. For nonorientable horseshoes, the set of border points consists of two points O_1 and O_2, in which case O_1 is s-border and O_2 is u-border. For half-orientable horseshoes with $b > 0$ [as in Fig. 2(a)] the set of border points consists of O_1 and O_2, and in this case O_1 is (s,u)-border while O_2 is u-border. For half-orientable horseshoes with $b < 0$ [as in Fig. 2(b)], the set of border points consists of the point O_1 and the 2-cycle P_2, and in this case O_1 is s-border while the points of the cycle P_2 are u-border.*

Apart from the set of (finitely many) border points, any horseshoe has the corresponding (countable) set of *endpoints*. Recall that for an interval Cantor set, the endpoints are the boundary points of its gaps. Accordingly, for a plane Cantor set which is the direct product of two interval Cantor sets, the endpoints are those points which are the product of the endpoints of the interval Cantor sets. Since horseshoes are homeomorphic to the direct product of (interval) Cantor sets, the notion of their endpoints is well defined. Moreover, horseshoes can be considered as dynamically defined Cantor sets [Palis & Takens, 1993]; this means that all endpoints are, in fact, the points of intersection for stable and unstable manifolds of s-border and u-border points. Thus, the set of endpoints coincides with the set of corresponding heteroclinic orbits (and/or homoclinic orbits whenever (s,u)-border points exist). In these terms, Theorem 2 can be rewritten as follows.

Corollary 1. *For orientable horseshoes of GHMs, the set of endpoints coincides with all homoclinic points to O_1. For nonorientable horseshoes, the set of endpoints coincides with all heteroclinic points from O_2 to O_1. For half-orientable horseshoes of simple type with $b > 0$ [as in Fig. 2(a)], the set of endpoints consists of all homoclinic points to O_1 and all heteroclinic points from O_2 to O_1. For half-orientable horseshoes of simple type with $b < 0$ [as in Fig. 2(b)], the set of endpoints consists of all heteroclinic points from P_2 to O_1.*

See Figs. 7–11 which illustrate Theorem 2 and the corollary.

Now we state our results on more interesting half-orientable horseshoes for GHM (5), i.e. on half-orientable horseshoes other than the simple ones. As we said before, the Jacobian J of (5) vanishes on the line $y = b/\alpha$. If this line does not intersect Λ, then the collapse point lies in a Cantor gap and Λ is still a horseshoe but it has different orientation for $y < b/\alpha$ and $y > b/\alpha$. The following

result describes bifurcations related to the appearance (resp. destruction) of such horseshoes.

Theorem 3. *Let $\gamma > 4$ be fixed. Then in any sufficiently small neighborhood V of the origin in the (α, b)-plane, there exists a domain*

$$\hat{D} \equiv \left\{(\alpha, b) : 0 < \frac{b}{\alpha} < 1 + \rho(\alpha, b)\right\} \qquad (6)$$

with $\rho(\alpha, b) \to 0$ as $\alpha, b \to 0$. This domain contains the origin and the following holds:

1. *If $(\alpha, b) \in V \backslash \hat{D}$, the map $\hat{T}(\gamma, b, \alpha)$ has the Smale horseshoe, which is orientable for $b > 0$ and nonorientable for $b < 0$;*
2. *The domain $\hat{D}$ contains infinitely many open cone regions adjoined to the origin, and in each of these regions the map $\hat{T}$ has a half-orientable horseshoe*;
3. *The boundary $b = 0$ of $\hat{D}$ corresponds to the first bifurcation, when the collapse point P^* coincides with the fixed point O_1 and, thus, O_1 has zero multiplier*;
4. *The boundary $b = \alpha(1 + \rho(\alpha, b))$ corresponds to the last bifurcation, when the collapse point becomes (at the last moment) homoclinic to O_1.*

Theorem 3 is illustrated in Fig. 4, where the corresponding bifurcation moments are shown: for the first bifurcation, at $b = 0$, see Figs. 4(d) and 4(h) and for the last bifurcation, at $b/\alpha = 1 + \rho(\alpha, b)$, see Figs. 4(b) and 4(f). The proof of Theorem 3 and related details are given in Sec. 5.

Note that in the case under consideration (i.e. when α and b are small, $\gamma > 4$), the mentioned bifurcations do not destroy essentially the hyperbolic structure. All these bifurcations are "instant": just before and just after such a bifurcation, the

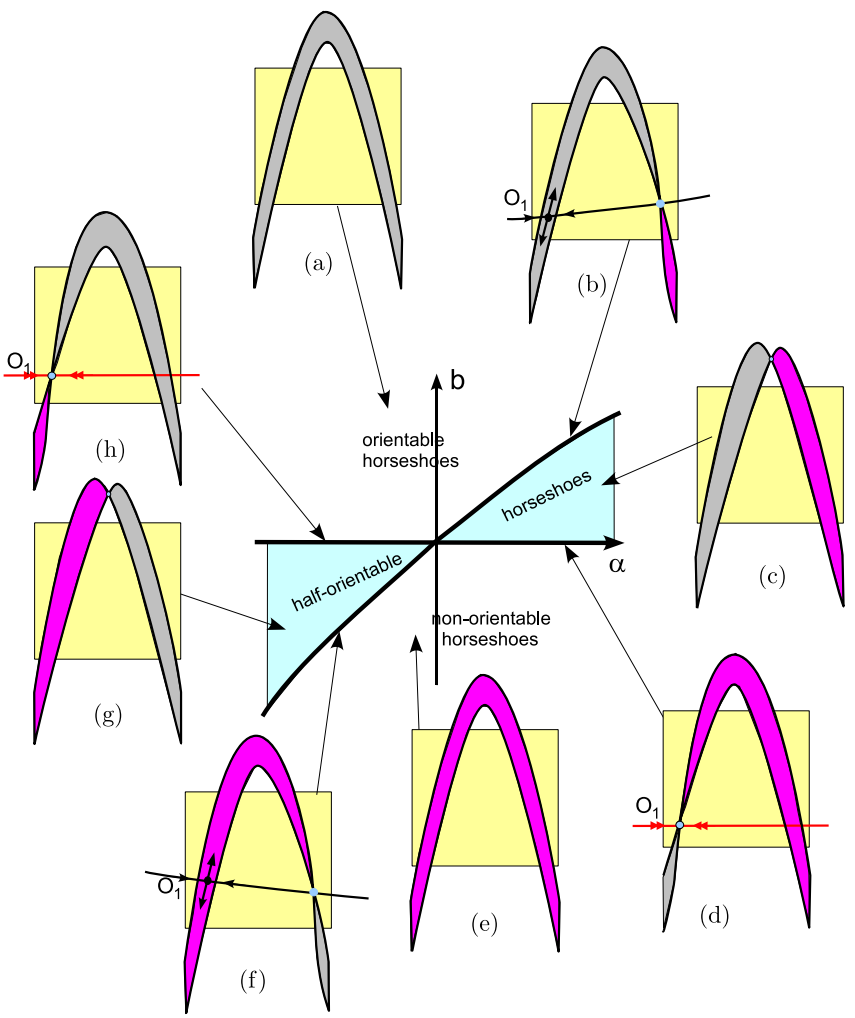

Fig. 4.

nonwandering set is still the horseshoe conjugate to $\mathcal{B}_2$ and all unstable manifolds of the horseshoe intersect at the collapse point. Before the bifurcation, the collapse point P^* is wandering, but at the bifurcation moment, it becomes nonwandering and thus, at this moment we have a "degenerate horseshoe" with infinitely many points (which belong to the line $y = b/\alpha$) being mapped into P^*. Thus, infinitely many orbits which have been glued into the collapse point, have the same forward semi-orbit. Of course, such a situation is impossible for the usual Smale horseshoe.

Our considerations will imply the following general result on a variety of half-orientable horseshoes.

Proposition 1. *There are infinitely many classes of half-orientable horseshoes with respect to the local equivalence relation.*

Proposition 1 is a consequence of the following theorem which states that by bifurcations near the line $b = 0$ in the parameter plane, the border points for GHMs may get unbounded periods, and thus, there are infinitely many classes of half-orientable horseshoes, because periods of border points are invariants for the local conjugacy. For more definiteness, let us consider a one-parameter family of maps $\hat{T}$ with $\alpha = \alpha_0 < 0$ and $\gamma > 4$ fixed. We take b as the parameter varying in a small interval $(-\epsilon, +\epsilon)$.

Theorem 4. *For any $\varepsilon > 0$ there is a sequence $\delta_n \subset (-\epsilon, 0)$ of disjoint intervals accumulating to 0 as $n \to \infty$, such that the map $\hat{T}$ with parameters $\alpha = \alpha_0, \gamma > 4$ and $b \in \delta_n$ has a half-orientable horseshoe $\Lambda(\alpha, b, \gamma)$ which possesses a u-border periodic point of period q_n. Moreover, $q_n \to \infty$ as $n \to \infty$.*

Proof. The proof is based on the observation that there are countably many values $b = b_n$ which correspond to border points for $T = T_{b_n}$ of periods s_n with $s_n \to \infty$. See Fig. 5 which illustrates the mentioned observation. Indeed, note that in the case when $b > 0$ we have the orientable Smale horseshoe, and thus, in this case the manifold $W^u(O_1)$ forms the boundary of Λ; so, by Theorem 2, the fixed point O_1 is (s, u)-border one. However, when $b < 0$, the point O_1 fails to be u-border, since its stable multiplier becomes negative. Bifurcation at the moment $b = 0$ leads to certain reconstructions in the set of periodic orbits, and, as a result, some points of these orbits are posed from both sides of $W^u_{\rm loc}(O_1)$ (see points p_1 and p_2 in Fig. 5, here a period four orbit is shown as u-border). Moreover, some of them become u-border because their unstable manifolds surround $W^u(O_1)$ from the left and from the right. Note that this reconstruction influences only those periodic points which visit a sufficiently small neighborhood of O_1, and such a neighborhood vanishes as the distance between the collapse point P^* and O_1 tends to zero (i.e. as $b \to -0$). Periods of these periodic points (except for O_1), in any horseshoe, tend to infinity as the diameter of the neighborhood under consideration tend to zero. Thus, we have that periods of u-boundary points tend to ∞ as $b \to -0$. ■

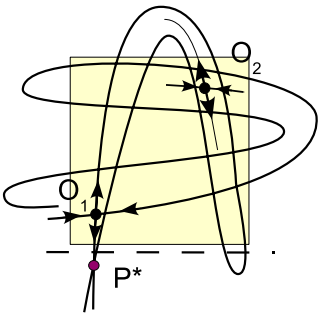

(a)

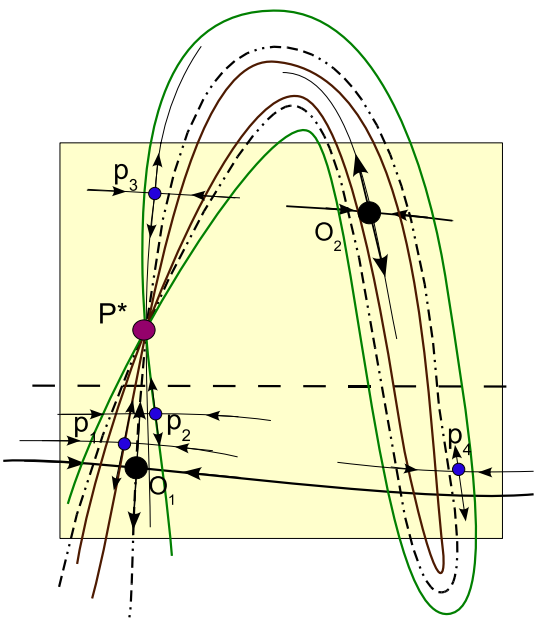

(b)

Fig. 5.

Theorem 4 gives us immediately the following.

Corollary 2. *Analytical endomorphisms of the disk can have (half-orientable) horseshoes of infinitely many different topological types.*

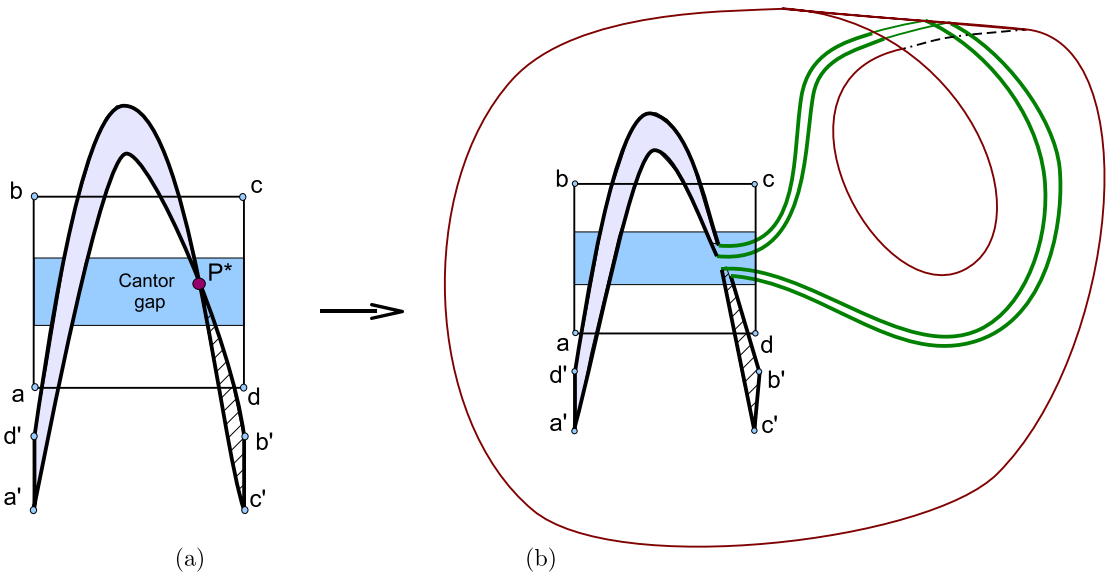

Fig. 6.

Moreover, we can realize every such horseshoe for diffeomorphisms of nonorientable two-dimensional manifolds. It can be easily created using a quite simple surgical construction, like that shown in Fig. 6 for the case of the Möbius band. Here, we start from an initial endomorphism of the disk which has a half-orientable horseshoe of the given type and obtain, after the "surgery", a diffeomorphism possessing the same horseshoe.

Corollary 3. *C^∞-diffeomorphisms on any two-dimensional nonorientable manifold can have (half-orientable) horseshoes of infinitely many different topological types.*

The paper is organized as follows. In Sec. 2, we describe the construction of Smale horseshoes with emphasis on their border points and end points; this gives us the proof of Theorem 2 concerning orientable and nonorientable horseshoes. In Sec. 3, we study hyperbolic dynamics of GHMs and we complete the proof of Theorem 2 on half-orientable horseshoes. Theorem 1 is proved as Lemmas 1–3 of Sec. 4. The existence part of Theorem 3 is proved as Propositions 1 and 2 of Sec. 4, while the bifurcation part is proved (among other reconstruction details) in Sec. 5.

2. Smale Horseshoes in the Hénon Family

In this section, which serves also as a background, we give a brief description of well-known results related to hyperbolic properties of the Hénon map (see [Devaney & Nitecki, 1979] for instance). These results represent, in fact, the first part of Theorem 2, which concerns orientable and nonorientable Smale horseshoes by paying attention to their border points.

We consider the Hénon map in the parabola-like form

$$\overline{x} = y, \quad \overline{y} = \gamma y(1-y) - bx \tag{7}$$

(compare with (5)). If $b = 0$, the Hénon map degenerates into a quadratic map of the form

$$\overline{x} = y, \quad \overline{y} = \gamma y(1-y). \tag{8}$$

In fact, map (8) is one-dimensional. Indeed, every point from $\mathbb{R}^2$ after one iteration enters the invariant curve $y = \gamma x(1-x)$ and then it always remains there governed by the low $\overline{y} = \gamma y(1-y)$. The latter map is well-known in the one-dimensional dynamics as the logistic (or parabola) map. The nonwandering set $\tilde{\Lambda}(\gamma)$ of this map is contained in the interval $[0,1]$ for all (positive) γ. If $\gamma > 4$, then $\tilde{\Lambda}(\gamma)$ is a Cantor set, and the restriction of the map on $\tilde{\Lambda}(\gamma)$ is conjugate to the one-sided Bernoulli shift with two symbols, denoted by $\mathcal{B}_{2+}$. Formally speaking, we may claim hyperbolicity here only within the one-dimensional setting (see Sec. 2 of Chapter III in [de Melo & van Strien, 1993] for agreements in the definition of hyperbolicity for one-dimensional maps). If b becomes nonzero (again with $\gamma > 4$) then $\tilde{\Lambda}(\gamma)$ becomes the regular

hyperbolic set for (7), let us denote it by $\Lambda(b,\gamma)$; so $\Lambda(b,\gamma)$ is the usual Smale horseshoe.

However, the horseshoes $\Lambda = \Lambda(b,\gamma)$ with $b > 0$ and $b < 0$ have different geometrical structures. Indeed, if $b > 0$ the horseshoe is orientable, and if $b < 0$ it is nonorientable, see Fig. 1. Moreover, these horseshoes may serve as dynamically defined Cantor sets [Palis & Takens, 1993], so there are other dynamical characteristics distinguishing horseshoes. One of them is the dynamical type of border points.

In fact, the set Λ has a geometrical structure of the planar Cantor set K_{xy} that is the direct product of two interval Cantor sets K_x and K_y (horizontal and vertical ones, respectively). The border points of Λ are those periodic points whose corresponding invariant manifolds (stable and unstable ones for s-border and u-border points, respectively) serve as one-dimensional boundaries for Λ. Thus, these manifolds project to the endpoints of the gaps for the interval Cantor sets (homeomorphic to K_x and K_y, respectively). So one can construct the interval Cantor set homeomorphic to K_y (resp. K_x) by the procedure of continuation of stable (resp. unstable) manifolds for s-border (resp. u-border) points. Thus, the border points produce the endpoints of Λ, and due to the described procedure, these endpoints are homoclinic and/or heteroclinic to the corresponding border periodic points.

We illustrate now the above procedure for the Hénon family. In *the orientable case* the fixed point O_1 has positive multipliers, hence its stable and unstable manifolds form the boundaries of Λ. In Fig. 7 the first two steps of the Cantor procedure are shown. First, the initial square $\overline{Q}$ is created, its sides are the corresponding pieces of the stable and unstable manifolds of point O_1, see Fig. 7(a). The sides $[O_1, h_3]$ (or $[h_1, h_2]$) and $[O_1, h_1]$ (or $[h_2, h_3]$) can be regarded as the initial segments for the sets K_x and K_y. Note that all endpoints of these segments, $\{O_1, h_1, h_2, h_3\}$, are nonwandering and belong to Λ.

The second step is shown in Fig. 7(b), where some middle gaps are removed from the segments K_x and K_y by a simple continuation of the pieces of $W^s(O_1)$ and $W^u(O_2)$. The rest set consists of four squares $Q_{00}, Q_{01}, Q_{10}, Q_{11}$ belonging to $\overline{Q}$ and containing Λ inside. Moreover, the 16 vertices of these four squares are point O_1 and 15 points homoclinic to it. These 16 points are the result of the product of four endpoints of K_x and four endpoints of K_y. Next, iterations of the sides of Q_{ij} lead to new boundaries for Λ inside Q_{ij}, etc. Note that the other fixed point of the map, O_2, has both multipliers negative and is posed inside Q_{11}. Thus, the fixed

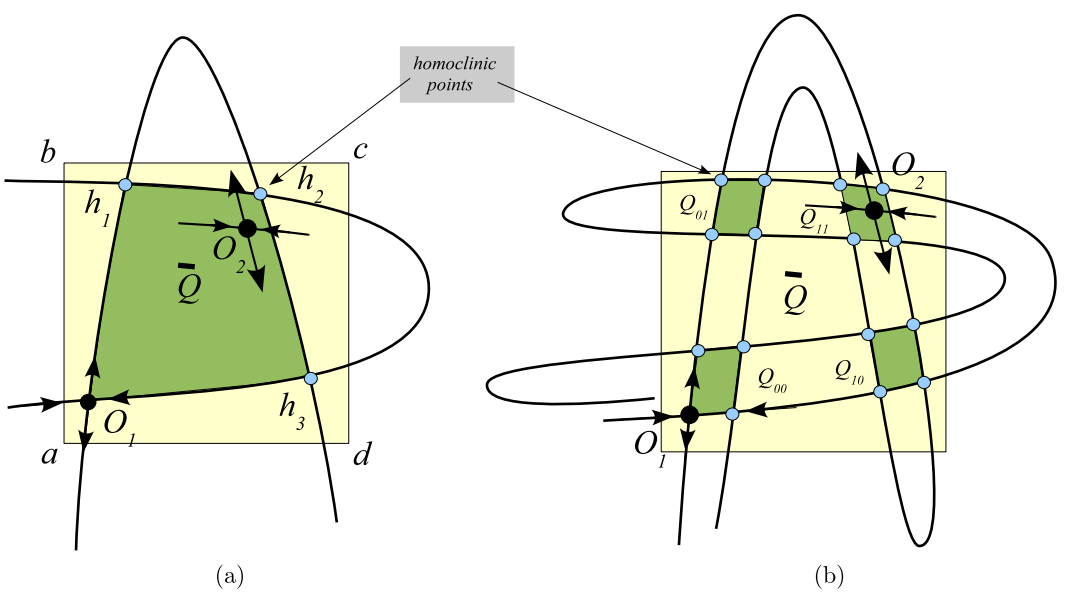

Fig. 7. The beginning of the Cantor procedure for the orientable Smale horseshoe. (a) Some initial pieces of the stable and unstable manifolds of O_1 form a curvilinear square $\overline{Q}$ such that (i) there are no nonwandering points outside $\overline{Q}$; (ii) some points of orbits from Λ belong to the boundary of $\overline{Q}$ (four such points are depicted in the figure: three of them are homoclinic points, (h_1, h_2, h_3), and one is the fixed point O_1). (b) Continuation of the pieces of $W^s(O_1)$ and $W^u(O_1)$ forms four new squares Q_{00}, Q_{01}, Q_{10} and Q_{11} such that there are no nonwandering points outside them and the vertexes of these squares correspond to 16 nonwandering points (15 homoclinic ones and the fixed point O_1).

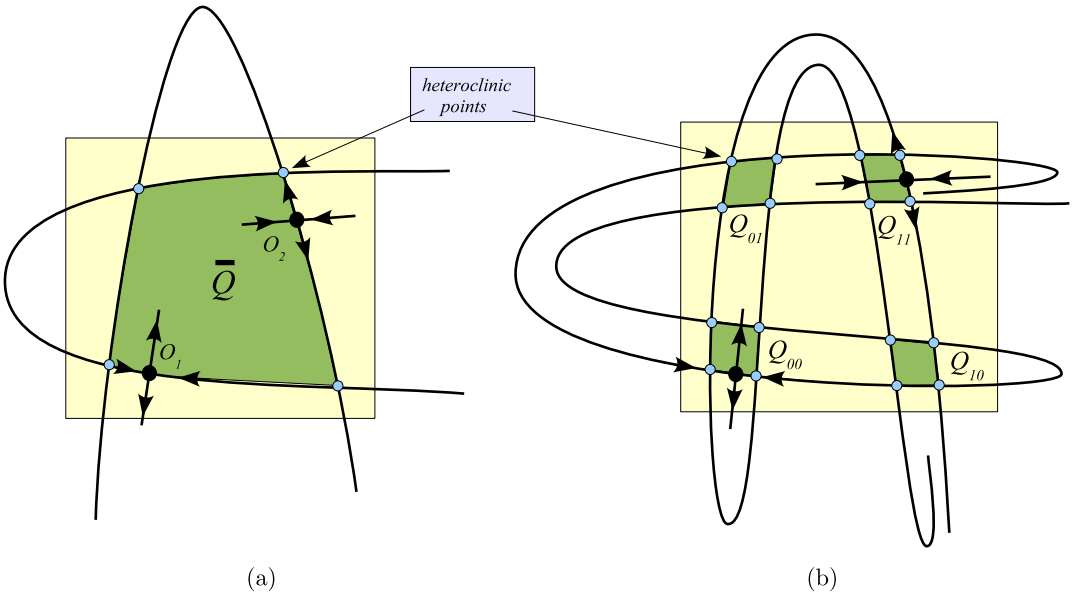

Fig. 8. The beginning of the Cantor procedure for the nonorientable Smale horseshoe.

point O_1 is (s,u)-border, and this point together with all its homoclinic points compose the set of endpoints of the Cantor set $K_{xy} := \Lambda$.

In *the nonorientable case* the fixed point O_1 has positive unstable and negative stable multipliers; the other fixed point O_2 has negative unstable and positive stable multipliers. Thus, the unstable manifold of O_1 cannot form the boundary, since points of some orbits from Λ accumulate to it from both sides. Nevertheless, the stable manifold $W^s(O_1)$, as before, forms the horizontal boundary for Λ. Other boundaries, vertical, are created by the unstable manifold of the fixed point O_2. So in this case, O_1 is s-border and O_2 is u-border, and thus, the set of endpoints for K_{xy} is exactly the set of all heteroclinic points between saddles O_2 and O_1. In Fig. 8, the first two steps of this Cantor procedure are shown. First, the initial square $\overline{Q}$ is created, its sides are the corresponding pieces of $W^s(O_1)$ and $W^u(O_2)$. The vertices of this square are specific points of the heteroclinic orbits between O_2 and O_1; points of such an orbit tend to O_1 (resp. O_2) under forward (resp. backward) iterates of the map. The second step is shown in Fig. 8(b), where some middle gaps are removed from the segments K_x and K_y by the procedure of continuation of the pieces $W^s(O_1)$ and $W^u(O_2)$. The rest set consists of four squares belonging to $\overline{Q}$ with points of Λ inside these squares (or on their sides). Moreover, the vertexes of these squares are 16 specific heteroclinic points. Note that in this case, both O_1 and O_2 are not the endpoints of K_{xy}, because their projections are not border points of K_x and K_y, respectively.

It is well known that both types of Smale horseshoes are observed in the standard Hénon map: the orientable ones occur for $b > 0$ and nonorientable ones for $b < 0$. As b varies from positive to negative values, the type of corresponding horseshoes is changed too. However, the transition is singular, because at $b = 0$ the Hénon map becomes one-dimensional and has no inverse. At the transition through $b = 0$ an immediate "switch" of the horseshoe geometry takes place. Indeed, the preimage $T^{-1}(Q)$ has (for $b \neq 0$) a horseshoe form. However, the tops of horseshoes $T^{-1}(Q)$ will be posed differently for $b > 0$ and $b < 0$, see Fig. 1. Moreover, it is easily seen that the x-coordinate of the tops tends to ∞ as $b \to 0$; namely, it tends to $+\infty$ (resp. $-\infty$) as $b \to +0$ (resp. $b \to -0$).

3. Existence of Half-Orientable Horseshoes for GHMs

In this section we study hyperbolic dynamics of GHMs in form (5). We will consider α and b as parameters varying near zero,[3] they might be

[3]In fact, it is enough to assume that both b and α tend to 0 as $\gamma \to 4$. However, for the "sample" value $\gamma = 6$ we may consider b and α less than $1/2$ in the absolute value, see Sec. 4.

positive, negative and zero as well. Moreover, we will suppose the coefficient γ to be fixed and besides, $\gamma > 4$. As a result, we will complete the proof of Theorem 2 for half-orientable horseshoes.

3.1. *Half-orientable horseshoes of simple type in GHM*

In this subsection we consider the case when b and α satisfy the condition $\alpha = 2b$. Note that the Jacobian of map (5) is

$$J \equiv b - \alpha y, \tag{9}$$

and, thus, J vanishes on the line $y = 1/2$. Also, the inverse map to (5) can be written in the following form

$$y = \overline{x}, \quad x = \frac{\gamma\overline{x}(1-\overline{x}) - \overline{y}}{b - \alpha\overline{x}}. \tag{10}$$

Thus, this map is well defined, except for the line $\overline{x} = b/\alpha = 1/2$. Note that, if $\gamma > 4$, the lines $y = 1/2$ and $x = 1/2$ are away from (uniform) hyperbolic dynamics demonstrated by map (5) for sufficiently small b and α. It relates also to the Hénon map (7) for $\gamma > 4$ and small b (see [Afraimovich & Hsu, 2002] and Sec. 4).

For the one-dimensional parabola map (8), its nonwandering set is posed inside the unit square $Q_0 = [0,1] \times [0,1]$. For map (5) and the corresponding Hénon map (7), both with $\gamma > 4$, we consider a slightly bigger square $Q_\beta = [-\beta, 1+\beta] \times [-\beta, 1+\beta]$, where $\beta \to 0$ as α and b tend to 0; for example, $\beta = (|\alpha| + |b|)/2$ is a sufficient quantity for us. For the Hénon map (7), the shape of Q_β, $\hat{T}(Q_\beta)$ and $\hat{T}^{-1}(Q_\beta)$ looks like in Fig. 1(a) for $b > 0$ and in Fig. 1(b) for $b < 0$, so map (7) remains, geometrically, the usual horseshoe map.[4] However, for GHMs (5) we have rather different pictures, see Figs. 9(a) and 9(b), where the new horseshoe geometry is shown. We can see that the GHM map $\hat{T} : Q \mapsto \hat{T}(Q)$ changes the orientation at a singular point P^*, which is the image of the line $y = 1/2$ (recall that $J(\hat{T})$ with $\alpha = 2b$ vanishes on this line). So the image $\hat{T}(Q)$ of the square Q forms a twisted band. As a result, map $\hat{T}$ has different orientations on the half-planes $y > 1/2$ and $y < 1/2$. Also, in these cases the inverse map $\hat{T}^{-1}$ is discontinuous on Q: it is not defined on the line $x = 1/2$. As a result, the set $\hat{T}^{-1}(Q \backslash \{x = 1/2\})$ forms two (infinitely long) strips that tend asymptotically to the line $y = 1/2$, and the asymptotic directions are opposite for the cases in Figs. 9(a) and 9(b). Nevertheless, the action of map $\hat{T}$ in both cases looks geometrically like in the case of a horseshoe map, and we will refer to such horseshoes (i.e. to those which have the collapse point P^* above the square Q) as of half-orientable horseshoes of simple type (in contrast to half-orientable horseshoes like in Figs. 2(c) and 2(d) mentioned also in Theorems 3 and 4).

3.2. *Border points of half-orientable horseshoes of simple type*

We saw that Smale horseshoes in orientable and nonorientable cases have different types of border points. The same can be observed for half-orientable horseshoes, as is shown in this subsection for horseshoes of simple types.

Consider first horseshoes like in Fig. 9(a). There is a horizontal line s_0 (for example, $y = 1/2$ as in the previous section), which is mapped under $\hat{T}$ into the collapse point P^* (posed in upper Q when $\gamma > 4$ and relation $\alpha = 2b$ holds for sufficiently small b and α). Denote its intersection points with the vertical sides $[a, b]$ and $[c, d]$ by s_0^1 and s_0^2 respectively. The square Q is divided by s_0 into two parts D_0 and D_1 lying, respectively, below and above s_0. Denote by a', d', b', c', the images under $\hat{T}$ of the corresponding vertices of Q. Note that $\hat{T}(s_0) = P^*$ and, thus, $\hat{T}(s_0^1) = \hat{T}(s_0^2) = P^*$. Map $\hat{T}$ is orientable on D_0 and nonorientable on D_1. This means that directions of the corresponding rounds for D_0 (i.e. $a \to d \to s_{02} \to s_{01} \to a$) and $\hat{T}(D_0)$ (i.e. $a' \to d' \to P^* \to a'$) are the same, whereas, the rounds for D_1 (i.e. $b \to c \to s_{02} \to s_{01} \to b$) and $\hat{T}(D_1)$ (i.e. $b' \to c' \to P^* \to b'$) are opposite [see Fig. 9(a)].

Now we indicate the border points. First, we construct invariant boundaries for Λ composed from some unstable manifolds of Λ. To attain this goal, we look for the behavior of sides $[a, b]$ and $[c, d]$ of Q under iterations of $\hat{T}$. We see that $\hat{T}([a, s_0^1])$ covers over the left part of Q along the y-coordinate, the same is true for the curve $\hat{T}([a, s_0^1])$, etc. Since map $\hat{T}|_Q$ is strongly expanding with respect to the y-coordinate, it follows that iterations of $[a, b]$

[4]For $\gamma = 6$ it is straightforward to check that the map is hyperbolic if, for example, $|b| < 1/2$; anyway, one can examine sufficient conditions of hyperbolicity, which are described in [Afraimovich *et al.*, 1977, 1983] or in Lemma 2 below.

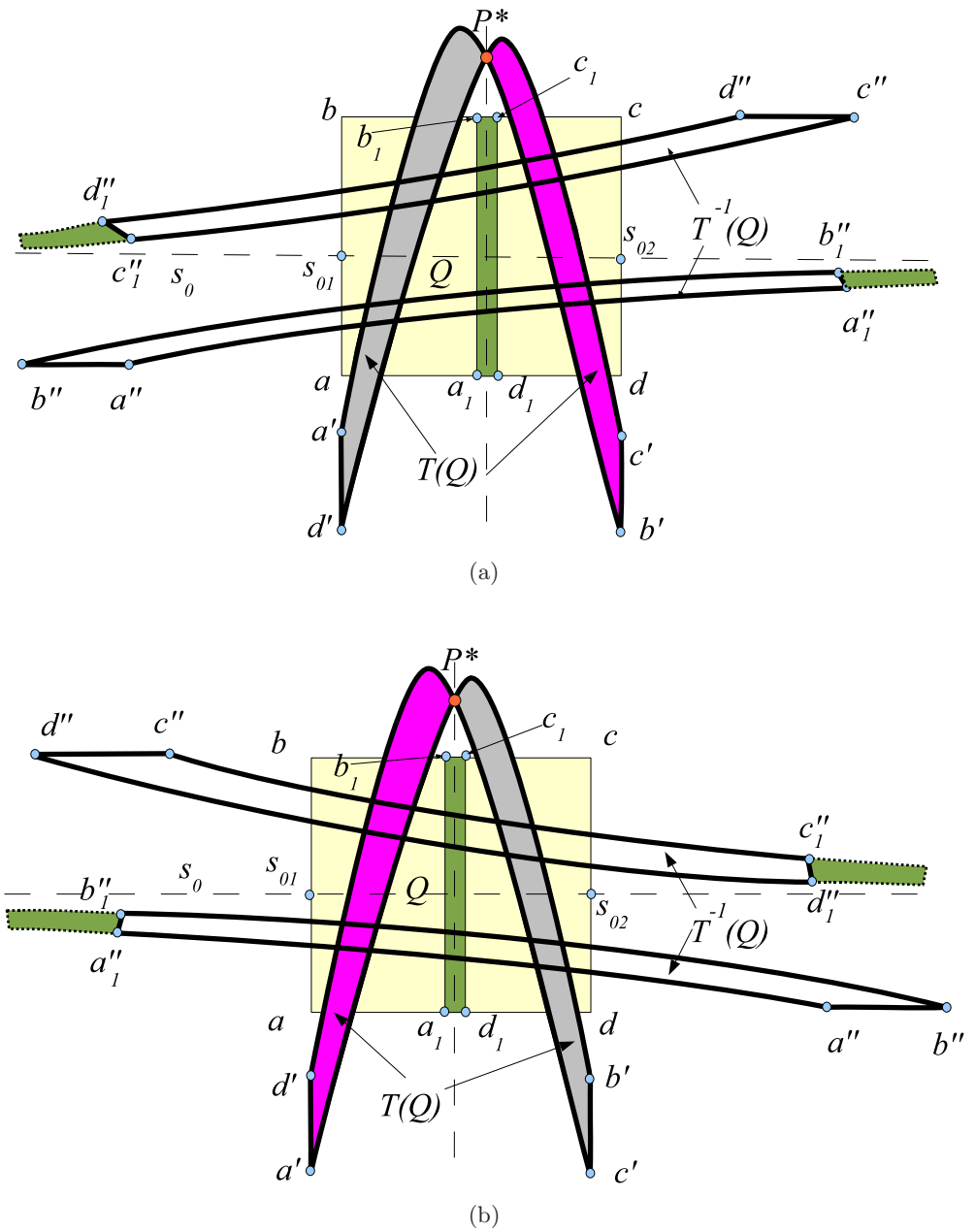

Fig. 9. Half-orientable horseshoes of simple type for GHM (5) in the cases: (a) $b > 0$, and (b) $b < 0$. The orientable part of the horseshoes is the left one (resp. the right one) for case (a) (resp. for case (b)).

accumulate (from the left) to some invariant curve of Λ containing the fixed point O_1. Thus, the left invariant boundary for Λ is the connected component of $W^u(O_1)$ containing the point O_1. It is shown analogously that the right invariant boundary for Λ is the connected component of $W^u(O_2)$ containing the point O_2. So map $\hat{T}$ acts on D_0 (resp. on D_1) in the same manner as in the orientable (resp. nonorientable) case. However, due to the presence of the collapse point P^* both outside pieces of manifolds $W^u(O_1)$ and $W^u(O_2)$ become, automatically, inner right and left, respectively, boundaries for Λ, see Fig. 9(a). Also we can similarly construct upper, lower, inner upper and inner lower boundaries consisting of some pieces of stable manifolds.

Now we construct invariant boundaries of Λ composed from some stable manifolds of Λ. In Fig. 9(a), the action of map $\hat{T}^{-1}$ on Q is also depicted. This map is discontinuous at $x = 1/2$. Therefore, we take off some rectangle R_1 with vertexes a_1, b_1, c_1, d_1 from Q (note that all points from R_1 are wandering). As a result, the image

$\hat{T}^{-1}(Q\backslash R_1)$ consists of two strips stretched in the x-direction and intersecting regularly D_0 and D_1. The image of the segment $[a, a_1]$ is the lower side of the lower strip. It follows that iterations of $[a, a_1]$ under $\hat{T}^{-1}$ will accumulate to the stable manifold of the fixed point O_1. Hence, the lower invariant boundary of Λ is the connected (in Q) component of $W^s(O_1)$ containing the point O_1. Its image under $\hat{T}^{-1}$ is the upper boundary, since the segment $[d_1, d]$ is mapped into the line $[d_1', d']$ that is the upper boundary of $\hat{T}^{-1}(Q\backslash R_1)$. Also, it is easily seen that the upper and lower inner invariant boundaries for Λ are the corresponding pieces of $W^s(O_1)$. Thus, in this case the set of endpoints of Λ consists exactly of all homoclinic points to O_1, all heteroclinic points from O_2 to O_1 and the fixed point O_1, see Fig. 10. The point O_2 is not the endpoint, since it is not such a point for K_y, while O_2 and O_1 are, respectively, u-border and (s, u)-border points for Λ.

Consider now half-orientable horseshoes like in Fig. 9(b). Here the map $\hat{T}$ is nonorientable on D_0 and orientable on D_1, thus, images of the vertex points of Q, lying from below Q, are ordered as d', a', c', b'.

Now we indicate the border points. Note that in this case both manifolds $W^u(O_1)$ and $W^u(O_2)$ cannot play the role of boundaries, since points O_1 and O_2 have negative stable multipliers and, thus, some points of Λ will accumulate to these manifolds from both sides. This can be seen by analyzing the behavior of sides $[a, b]$ and $[c, d]$ of Q under iterations of $\hat{T}$. Indeed, the image $\hat{T}([a, s_0^1])$ is not now the left boundary of $\hat{T}(Q)$, while the image $\hat{T}([c, s_0^2])$ is not now the right boundary. However, $\hat{T}([b, s_0^1])$ and $\hat{T}([d, s_0^2])$ are, respectively, the left and the right boundaries of $\hat{T}(Q)$. Moreover, $\hat{T}([b, s_0^1])$

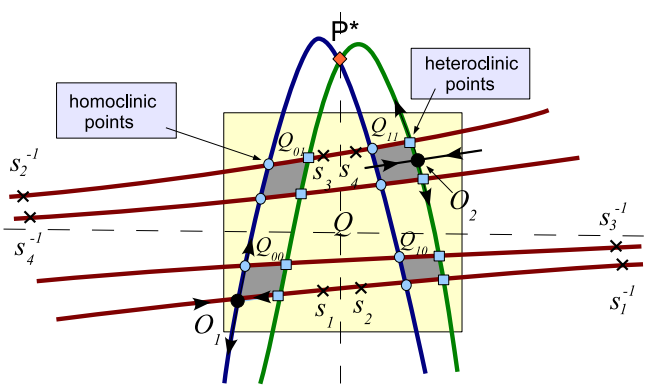

Fig. 10.

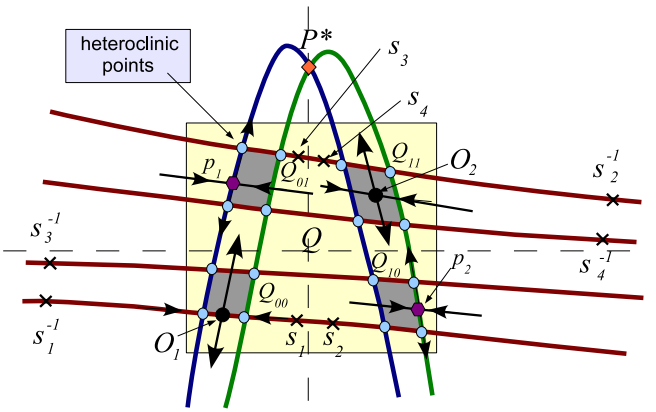

Fig. 11.

(resp. $\hat{T}([d, s_0^2])$) covers the right part (resp. the left one) of Q along the y-coordinate. Thus, the second iteration of each of these segments covers itself, hence there is a period-2 orbit, say P_2. It follows that the left and right invariant boundaries for Λ are the corresponding connected pieces of the unstable manifold of the period-2 orbit P_2. There is such a unique orbit in any horseshoe. The inner left and right invariant boundaries are again the corresponding connected pieces of $W^u(P_2)$: it is sufficient to continue the left and right parts of $W^u(P_2)$ ahead of point P^* and the corresponding pieces will form (due to the switching near P^*) the left and right inner boundaries. Similarly, the upper and lower boundaries (outside and inside) form the corresponding pieces of $W^s(O_1)$, see Fig. 11. Thus, in the case under consideration the set of border points of Λ consists exactly of point O_1 and the period-two orbit P_2, which are s-border, and u-border, respectively. Accordingly, the set of endpoints of Λ consists of all heteroclinic points from P_2 to O_1, while the fixed points O_1, O_2 and the period-2 orbit P_2 do not belong to the set of endpoints.

3.3. *On half-orientable horseshoes of other types*

Now, let us consider a general case when the condition $\alpha = 2b$ is given up. Then, since the Jacobian $J(\hat{T})$ vanishes on the line $y = b/\alpha$, it follows that if this line does not intersect the square Q, one has a horseshoe map similar to the Hénon map, see Figs. 4(a) and 4(e). However, as the value b/α varies (say, from 0 to 1) new types of half-orientable horseshoes (with P^* inside Q) may appear. In Figs. 2(c) and 2(d), two examples of such horseshoes are

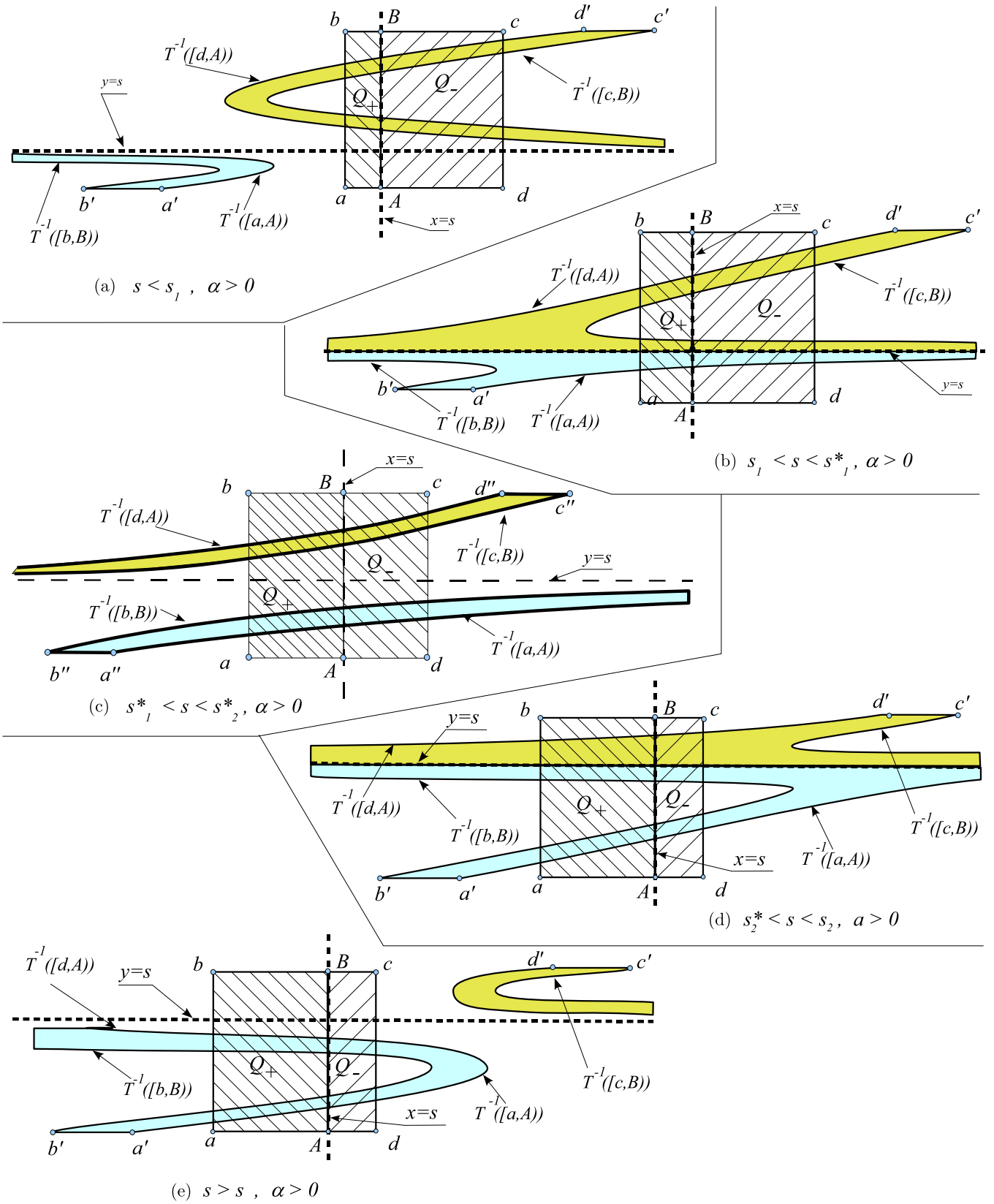

Fig. 12.

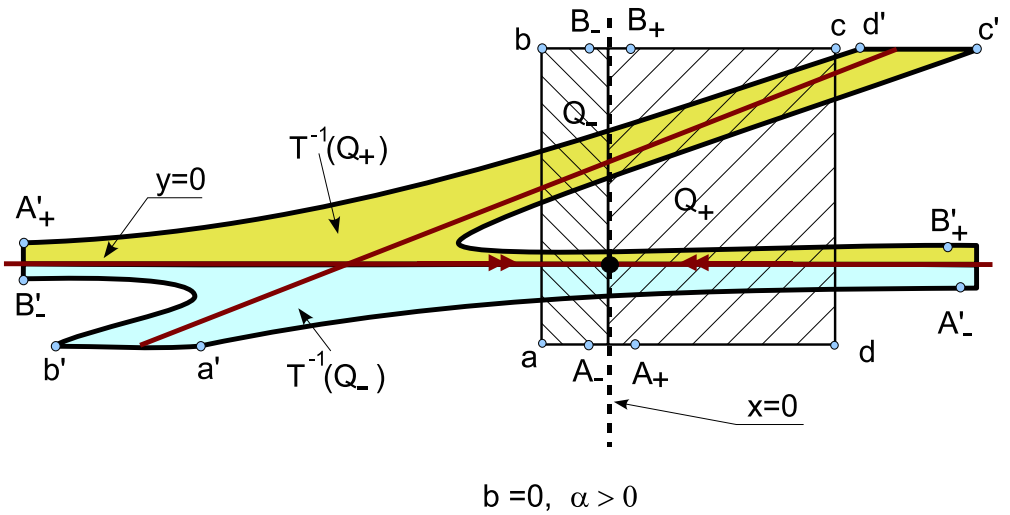

Fig. 13.

shown for the cases (a) $0 < b/\alpha < 1/2$; and (b) $1/2 < b/\alpha < 1$, with $b > 0, \alpha > 0$.

Note that when α and b vary (for fixed $\gamma > 4$), the corresponding reconstructions in the image $\hat{T}(Q)$ can be followed up without problems (see Fig. 4 which illustrates possible geometrical changes). However, the reconstructions in the preimage $\hat{T}^{-1}(Q)$ look rather nontrivial. The reason is that the map $\hat{T}^{-1}$ is discontinuous (on the line $x = b/\alpha$) and dependence on the parameters is singular in the sense that sharp reconstructions of the preimage $\hat{T}^{-1}(Q)$ occur as the parameters b and α vary near zero. We will trace the main steps of these reconstructions in Sec. 5, see Figs. 12 and 14 for an illustration. Note only that the pictures for $\hat{T}^{-1}(Q)$ in the case of half-orientable horseshoes from Figs. 2(c) and 2(d) will look as in Figs. 12(b) and 12(d), respectively.

4. Calculations for Half-Orientable Horseshoes

In this section we examine map (5) for sufficiently small values of the parameters b and α. If $\alpha = 0$, map (5) is the Hénon map of the form (7). It is well known that the latter map is hyperbolic for $\gamma > 4$ and all sufficiently small b: it has a Smale horseshoe (if $b = 0$, the map becomes one-dimensional and only conjugacy with $\mathcal{B}_{2+}$ takes place).[5] We need such results for the case GHM of the form (5). However, as we will show below, the standard horseshoes exist here not for all (sufficiently small) b and α, even for large γ.

Our first results deal with the "sample" case when the condition $\alpha = 2b$ holds and $\gamma = 6$. Then map (5) takes the form

$$\bar{x} = y, \quad \bar{y} = 6y(1-y) - bx + 2bxy. \tag{11}$$

In what follows, we will denote this map by $\tilde{T}$ or $\tilde{T}_b$.

Consider a square $Q_\beta = [-\beta, 1+\beta] \times [-\beta, 1+\beta]$ centered at the point $(1/2; 1/2)$. Denote the vertexes of Q_β by $a(-\beta; -\beta)$, $b(-\beta; 1+\beta)$, $c(1+\beta; -\beta)$ and $a(1+\beta; -\beta)$, and the sides of Q_β by $[a, b]$, $[b, c]$, $[c, d]$ and $[a, d]$.

Lemma 1. *For all sufficiently small $b \neq 0$, $\beta > 0$ with $\beta \to 0$ as $b \to 0$ such that*

(i) *the set $\tilde{T}_b(Q_\beta) \cap Q_\beta$ consists of two connected components;*
(ii) $\tilde{T}_b([a, d]) \cap Q_\beta = \emptyset$, $\tilde{T}_b([b, c]) \cap Q_\beta = \emptyset$;
(iii) *there is a rectangle $D_\beta \subset Q_\beta$ such that $\tilde{T}_b(D_\beta) \cap Q_\beta = \emptyset$ and D_β contains the segment $y = 1/2$.*

Proof. It follows from (11), the image $\tilde{T}_b([a, d])$ is the segment $[a', d']$, where

$$a' = (-\beta; -6\beta(1+\beta) + b\beta + 2b\beta^2),$$
$$d' = (-\beta; -6\beta(1+\beta) - b - 3b\beta - 2b\beta^2).$$

[5]There are various results on the hyperbolic properties of the Hénon map. Thus, for the classical Hénon map $\bar{x} = y$, $\bar{y} = 1 - bx - ay^2$ a sufficient condition for hyperbolicity could be stated as $a > 1/4(5 + 2\sqrt{5})(1 + |b|)^2$ [Devaney & Nitecki, 1979; Afraimovich, 1984]. This gives the well-known hyperbolicity condition: $\gamma > 2 + \sqrt{5}$ for small b.

Analogously, $\tilde{T}_b([b,c]) = [b',c']$, where

$$b' = (1+\beta; -6\beta(1+\beta) + b\beta - 2b\beta(1+\beta),$$
$$c' = (1+\beta; -6\beta(1+\beta) + b + 3b\beta + 2b\beta^2).$$

Thus, (ii) will be satisfied, if

$$-6\beta(1+\beta) + |b| + 3|b|\beta + 2|b|\beta^2 < -\beta.$$

For small B and β this inequality can be written as

$$\beta > \frac{|b|}{5} + O(\beta^2 + b^2),$$

which proves (ii).

Next, the curves $\tilde{T}_b([a,b])$ and $\tilde{T}_b([c,d])$ are defined by the equations

$$\begin{aligned}\tilde{T}_b([a,b]) &: y = 6x(1-x) + b\beta - 2b\beta x,\\ &\quad -\beta \le x \le 1+\beta,\\ \tilde{T}_b([c,d]) &: y = 6x(1-x) - b(1+\beta) + 2b(1+\beta)x,\\ &\quad -\beta \le x \le 1+\beta.\end{aligned} \tag{12}$$

They have an intersection point $P^*(x^*, y^*)$ with

$$x^* = \frac{1+2\beta}{2(1+4\beta)} = \frac{1}{2} + \beta + O(\beta^2), \quad y^* = \frac{3}{2} + O(\beta^2).$$

Since $y^* > 1+\beta$ for small β, (i) is proved.

It follows from (11) that the inequality $\overline{y} > 1+\beta$ will be valid for all $x \in [-\beta, 1+\beta]$ if

$$6y(1-y) - |b|(1+\beta) - 2|b|(1+\beta)y > 1+\beta.$$

This allows to define the needed rectangle D_β as follows

$$\left| y - \frac{1}{2} + \frac{|b|}{6} \right| < \frac{\sqrt{3}}{6}(1 - 2|b| - \beta) + O(b^2 + \beta^2),$$
$$-\beta \le x \le 1+\beta. \tag{13}$$

Note that for one-dimensional map $\overline{y} = 6y(1-y)$ (map (11) at $b = 0$) the corresponding interval is defined as

$$\frac{1}{2} - \frac{\sqrt{3}}{6} < y < \frac{1}{2} + \frac{\sqrt{3}}{6}$$

that corresponds to our result for $b = \beta = 0$. ■

Lemma 2. *For all sufficiently small $b \neq 0$, the map $\tilde{T}_b : Q_\beta \mapsto \mathbb{R}^2$ is hyperbolic.*

Proof. It is sufficient to check that the following hyperbolicity conditions from [Afraimovich *et al.*, 1977, 1983] (see also [Shilnikov *et al.*, 1998, 2001; Afraimovich & Hsu, 2002]) are fulfilled

$$\begin{aligned}&\text{(a) } \|f_x\| < 1,\\ &\text{(b) } \|g_y^{-1}\| < 1,\\ &\text{(c) } 1 - \|f_x\|\|g_y^{-1}\| > 2\sqrt{\|f_y \times g_y^{-1}\|\|g_x\|\|g_y^{-1}\|},\\ &\text{(d) } (1 - \|f_x\|)(1 - \|g_y^{-1}\|) > \|f_y \times g_y^{-1}\|\|g_x\|,\end{aligned} \tag{14}$$

where the subscripts mean differentiation with respect to the corresponding coordinates. Note that by Lemma 1 we may consider the above inequalities for points on $Q_\beta \backslash D_\beta$ only since points from D_β are wandering. Then we have for map $\tilde{T}_b$

$$f_x \equiv 0, \quad f_y \equiv 1, \quad g_x = -b + 2by,$$
$$g_y = 6(1-2y) + 2bx.$$

It follows from (13) that the following estimate

$$|1 - 2y| \ge \frac{\sqrt{3}}{6}(1-\beta) - \frac{|b|}{3}(l + \sqrt{3}) + O(b^2 + \beta^2) \tag{15}$$

holds for points from $Q_\beta \backslash D_\beta$. Then we have that

$$\begin{aligned}|g_y^{-1}| &= \frac{1}{|6(1-2y) + 2bx|}\\ &\le \frac{1}{\sqrt{3}(1-\beta) - 2|b|(1 + 2\sqrt{3} + \beta)} < 1\end{aligned}$$

on $Q_\beta \backslash D_\beta$ for all sufficiently small b and β. Thus, condition (b) in (14) holds. Other conditions are easily checked. ■

Denote the connected components of the set $Q_\beta \backslash D_\beta$ by D_β^0 for the lower one and by D_β^1 for the upper one.

Lemma 3. *For $b > 0$, the map $\tilde{T}_b$ is orientable on D_β^0 and nonorientable on D_β^1. For $b < 0$, otherwise, the map $\tilde{T}_b$ is nonorientable on D_β^0 and orientable on D_β^1.*

Proof. It follows from (11) that $J(\tilde{T}_b) = b(1-2y)$, where J is the Jacobian of the map $\tilde{T}_b$. By virtue of (15), $-\beta < y < 1/2$ for D_β^0 and $1/2 < y < 1+\beta$ for D_β^1. Thus $\text{sign}(J) = \text{sign}(b)$ for D_β^0 and $\text{sign}(J) = -\text{sign}(b)$ for D_β^1. ■

Lemmas 1 and 2 imply that the map $\tilde{T}_b$ has a horseshoe for any $b \neq 0$ sufficiently small. On the other hand, Lemma 3 states that this horseshoe is half-orientable, in contrast to the usual Smale horseshoes for the Hénon map.

Until now we had assumed mostly that for GHMs, the condition $\alpha = 2b$ was satisfied. Now we wish to give up this condition. So, we will examine a GHM (5) with $\gamma = 6$, denoting it by $\tilde{T}_{\alpha,b}$. Note that many obtained results (including Lemma 1 and estimates (14) from Lemma 2) can be proved for this more general case without any additional treatments (just by replacing the coefficient $2b$ by α). However, let us notice that, formally speaking, the statement of Lemma 2 on hyperbolicity is valid only in the case when the collapse point P^* is wandering (i.e. when $P^* \notin \Lambda$) : otherwise, we have to speak of "singular hyperbolicity".

However, application of Lemma 3 is now principally incorrect for some (sufficiently small) b and α. The point is that since the Jacobian of $T_{\alpha,b}$ equals $J(\tilde{T}_{\alpha,b}) = b - \alpha y$, the map $\tilde{T}_{\alpha,b}$ changes the orientability on the line $y = b/\alpha$, which depends on the parameters (in contrast to the constant line $y = 1/2$ before). So the situation is somewhat different from the previous one. Although geometrical properties (like those in Lemma 1) and hyperbolic ones (like estimates 14) take place here, we cannot claim now the existence of the horseshoe. The reason is that the map $\tilde{T}_{\alpha,b}$ is not invertible, and in particular, $\tilde{T}_{\alpha,b}$ may have periodic orbits with zero multipliers; furthermore, unstable manifolds of some periodic points need not be disjoint, in which case the intersection point is nonwandering. Note that even for 'sample' map (11), all unstable manifolds of points of the horseshoe intersect (at the collapse point P^*). However, in this case the intersection point does not belong to Q_β and, thus, it is wandering. The image of the line $y = b/\alpha$ is exactly one point

$$P^*(b,\alpha) = \frac{\beta}{\alpha}\left(1;\ 6\left(1 - \frac{\beta}{\alpha}\right)\right).$$

Thus, all unstable manifolds of the invariant set $\Lambda(\tilde{T}_{\alpha,b})$ intersect at this point. It is clear, that if both the line $y = b/\alpha$ and the point P^* do not belong to Q_β, then the set Λ is the usual Smale horseshoe, which is orientable whenever $b > 0$ and nonorientable whenever $b < 0$. This situation takes place if $b/\alpha > 1 + \beta$ or $b/\alpha < -\beta$ which implies the following result.

Proposition 2. *If one has either $b/\alpha > 1$ or $b/\alpha < 0$, then for all sufficiently small b and α, the map $\tilde{T}_{\alpha,b}$ possesses the Smale horseshoe, which is orientable whenever $b > 0$, and nonorientable whenever $b < 0$.*

We can generalize this result as follows. Let $G_i, i = 0, 1, \ldots$, be the gaps of the Cantor set generated by the parabola map $\overline{y} = 6y(1 - y)$.

Proposition 3. *Let $b/\alpha \in G_i$ for some i. Then, for all sufficiently small such b and α, the map $\tilde{T}_{\alpha,b}$ has a horseshoe in Q_β. If $b > 0$, this map is orientable for $y < b/\alpha$ and nonorientable for $y > b/\alpha$. If $b < 0$, otherwise, this map is nonorientable for $y < b/\alpha$ and orientable for $y > b/\alpha$.*

The proof is straightforward. We need only to control that the line $y = b/\alpha$ does not intersect points of Λ. But it follows evidently (for all sufficiently small b and α) from the fact that this line does not intersect points of the set $\Lambda(0, 0)$ (i.e. the invariant set on the curve $y = 6x(1 - x)$ for the parabola map $\overline{x} = y$, $\overline{y} = 6y(1 - y)$).

Proposition 3 can be extended to GHMs of the form (5) with $\gamma > 4$. For every such γ, the corresponding parabola map $\overline{y} = \gamma y(1-y)$ has an invariant Cantor set with gaps $G_i(\gamma)$ that can play the role of gaps G_i from Proposition 3 (though the proof for the general case $\gamma > 4$ is technically more complicated; the situation here is similar to the proof of hyperbolicity for the parabola map $\overline{y} = \gamma y(1 - y)$ for $\gamma > 4$ (see [Robinson, 1999]), comparing with a much simpler proof for $\gamma > 2 + \sqrt{5}$.)

Since gaps $G_i(\gamma)$ are all posed in the segment $[0, 1]$, it implies that map (5) with $\gamma > 4$ can have half-orientable horseshoes only for values of $s = b/\alpha$ belonging to some intervals $I_{b,\alpha} = (\nu_1, 1+\nu_2)$, where $\nu_i(b, \alpha) \to 0$ as $(b, \alpha) \to 0$. Moreover, we can indicate the exact bifurcation boundaries ν_1^* and ν_2^* of $I_{b,\alpha}$. Namely, ν_1^* equals 0 exactly, and this value corresponds to the "first bifurcation" when the collapse point P^* coincides with the fixed point O_1 [see Figs. 4(d) and 4(h)). The value $s = \nu_2^*$ corresponds to the "last bifurcation" when the collapse point P^* becomes a homoclinic point to O_1 [see Figs. 4(b) and 4(f)]. This moment can be defined exactly too, and it is not difficult to calculate the coordinates of P^*, namely, $P^* = b/\alpha(1; \gamma(1 - (b/\alpha)))$ (here P^* is the image of the line $y = b/\alpha$ under map (5)). The bifurcation value $s = \nu_2^*$ corresponds to the situation when the point P^* belongs to the lower component of the manifold $W^s(O_1)$. This component can be calculated (e.g. numerically) and, thus, one can find ν_2^*. In this way, for small b and α (and with $\gamma > 4$ as necessary condition), one gets $s = \nu_2^*$ corresponds to the equation

$$\frac{b}{\alpha} = 1 - \frac{\alpha}{\gamma^2} + O(\alpha^2).$$

Thus, we have defined the boundaries for the region of existence of half-orientable horseshoes. For fixed γ, this region on the (α, b)-plane has a form of a cone adjoining to the origin, see Fig. 4. This completes the proof of Theorem 3 and, in connection with the existence problems of this section, in the next section we will consider main reconstructions of the horseshoe geometry leading from orientable to nonorientable Smale horseshoes via half-orientable ones.

Remark 2. All previous considerations can be repeated with only mild corrections for the case of GHMs of the form $\overline{x} = y, \overline{y} = \gamma y(1-y) - bx + \alpha xy + \nu y^3$, with b, α and ν sufficiently small. The term νy^3 is conservative, it does not change the Jacobian J, because $J = b - \alpha y$ is the same as before. Moreover, the line $y = b/\alpha$ under action of the map collapses again to the point $P^* = b/\alpha(1; 6(1-(b/\alpha)) + \nu((b/\alpha))^2)$.

5. On Geometry of Horseshoes for GHM

In this section we study the geometry of GHMs which correspond to diagrams in Fig. 4. Our main attention, however, will be focused on the description of reconstructions in the preimages $T^{-1}(Q)$ when the parameters α and b vary. Note that the corresponding reconstructions in the images $T(Q)$ are much easier and can be observed in Fig. 4 (see also Fig. 2 in addition). We consider the "sample" case $\gamma = 6$ for more definiteness. Besides, we restrict ourselves to one-parameter analysis using the quantity $s = b/\alpha$ as the governing parameter. Then the map T in form (5) can be rewritten as

$$\overline{x} = y, \quad \overline{y} = 6y(1-y) - \alpha x(s-y), \tag{16}$$

where α is sufficiently small and fixed. Thus, two different cases appear here: $\alpha > 0$ and $\alpha < 0$. (We exclude the case $\alpha = 0$ because it corresponds to the Hénon map, which has no interesting reconstructions for horseshoes).

As it was shown above, half-orientable horseshoes may exist in GHMs (5) only for values $-\beta \leq s < 1 + \beta$ of the parameter s. When s changes within these bounds, it corresponds to the movement of parameters α and b in Fig. 4, either along the path $(e) \to (c) \to (a)$ for positive α, or along the path $(a) \to (g) \to (e)$ for negative α. Thus, if we consider both cases (fixed positive and negative α), we "cover" all the cases in Fig. 4.

The following Figs. 12 and 14 summarize our considerations for the cases $\alpha > 0$ and $\alpha < 0$, respectively. First, let us comment on these figures (mainly, Fig. 12), and, then, we will present the proofs.

In Fig. 12, we start from the domain which corresponds to the case (e) in Fig. 4. Here, map (16) has a nonorientable horseshoe as the nonwandering set, and the preimage $T^{-1}(Q)$ has either a horseshoe form whenever $s < -\beta$ (similar to that for the Hénon map with $b < 0$, see Fig. 1(b)), or consists of two disconnected horseshoe shape pieces whenever $-\beta < s < s_1 < 0$ (like those in Fig. 12(a)). The moment $s = s_1 < 0$ corresponds to an immediate transformation of the disconnected pieces into one connected piece. (Formally, it corresponds to the change of asymptotic behavior of the preimage $T^{-1}([a, A])$, where $[a, A]$ is a segment of the side $[a, d]$ of the square Q). As a result, we will have, for $s_1 < s < s_1^*$, the situation shown in Fig. 12(b). Here, the nonwandering set is a horseshoe that becomes half-orientable just as s takes a positive value. It is interesting that at the moment $s = 0$, we have a singular horseshoe $T(Q)$ from Fig. 4(d), and its preimage $T^{-1}(Q)$ is shown in Fig. 13. Here, the fixed point O_1 has zero multiplier and its stable manifold has two singular pieces (horizontal ones); then, as s changes, these pieces are immediately reconstructed. Note that the part of $T^{-1}(Q)$ below the stable manifold of O_1 is wandering for $s = 0$, but as s becomes positive, it immediately captures the point O_1 and some nonwandering orbits. Thus, the moment $s = 0$ corresponds to the birth of a half-orientable horseshoe. When s is positive and rather small, we have a horseshoe $T(Q)$ like in Fig. 2(c) [the preimage $T^{-1}(Q)$ has a form like in Fig. 12(b)]. However, when s increases, the preimage becomes like in Fig. 12(c), and this corresponds to a half-orientable horseshoe of the simple type. Further change of s leads to the appearance of half-orientable horseshoes like in Fig. 12(d) [or, which is the same, as in Fig. 2(d)], and finally, to the appearance of orientable horseshoes [Fig. 12(e)].

In Fig. 12, we show reconstructions which occur to preimages of the sides of square Q_β. The moments of such reconstructions can be calculated precisely, see below. However, they are caused by some global bifurcations connected with sharp reconstructions of (stable) invariant manifolds of fixed points. In particular, one can detect such moments as those when the collapse point P^* coincides consequently with the fixed point O_1 (for

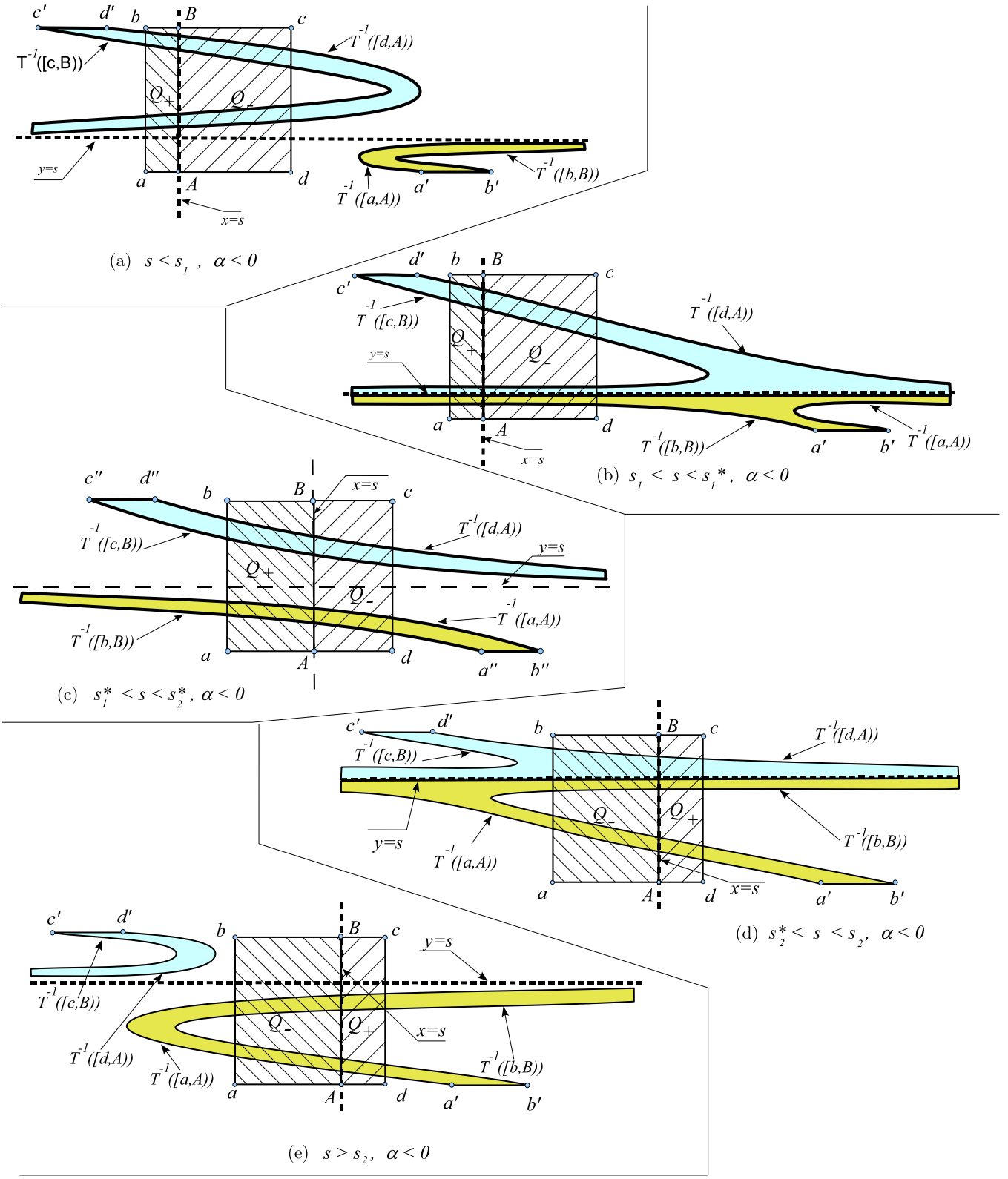

Fig. 14.

$s = 0$, namely), with the homoclinic points [see Fig. 7(a)] h_1, h_2 and h_3 (the last bifurcation).

In Fig. 14, the corresponding reconstructions are shown for the case $\alpha < 0$ when s varies from $-\beta$ to $1 + \beta$. This corresponds to the path $(a) \to (g) \to (e)$ in Fig. 4.

Now we provide the necessary calculations. The Jacobian of map (16) is equal to $J = \alpha(s - y)$. Thus, $J = 0$ at $y = s$. This implies that the map $T : Q_\beta \to \mathbb{R}^2$ is a diffeomorphism when either $s > 1+\beta$ or $s < -\beta$. In the first case (i.e. $s > 1+\beta$) the horseshoes are orientable if $\alpha > 0$, $b > 0$ and nonorientable if $\alpha < 0$, $b < 0$. In the second case (i.e. $s < -\beta$), the horseshoes are orientable if $\alpha < 0$, $b > 0$) and nonorientable if $\alpha > 0$, $b < 0$; see Figs. 4(a) and 4(e).

Now we suppose that $-\beta \le s \le 1+\beta$. Thus, the lines $y = s$ and $x = s$ intersect the square Q_β. The line $y = s$ divides Q_β into two rectangles D_0 and D_1 corresponding to $y < s$ and $y > s$, respectively. The map T has different types of orientability on D_0 and D_1, and the geometry of $T(Q_\beta)$ is rather simple, see Fig. 4. The line $y = s$ collapses into one point P^* that lies on the line $x = s$, so the images $T(D_0)$ and $T(D_1)$ (adjoining to P^*) have a triangle form. The construction of horseshoes for forward iterates in this case is geometrically similar to that in the case of the standard Smale horseshoe except when involving the collapse point and its forward images. However, the geometry of $T^{-1}(Q_\beta)$ could be rather nontrivial and it could change sharply as s varies. Below, we will study related problems.

The line $x = s$ (the line of discontinuity of T^{-1}) intersects the sides $[a, d]$ and $[b, c]$ at points A and B, respectively. Let us find the images, under the map T^{-1}, of the following intervals $[a, b]$, $[b, B)$, $[c, B)$, $[c, d]$, $[d, A)$ and $[a, A)$.

By (16), the map T^{-1} can be written in the following form

$$\overline{x} = \frac{6x(1-x) - y}{\alpha(s-x)}, \quad \overline{y} = x. \tag{17}$$

Thus, the images of vertices of square Q_β under T^{-1} are as follows

$$T^{-1}(a) = \left(\frac{-5\beta - 6\beta^2}{\alpha(s+\beta)}, -\beta\right),$$

$$T^{-1}(b) = \left(\frac{-1 - 7\beta - 6\beta^2}{\alpha(s+\beta)}, -\beta\right),$$

$$T^{-1}(c) = \left(\frac{-1 - 7\beta - 6\beta^2}{\alpha(s+\beta)}, 1+\beta\right),$$

$$T^{-1}(d) = \left(\frac{-5\beta - 6\beta^2}{\alpha(s+\beta)}, 1+\beta\right). \tag{18}$$

Now we find the images under T^{-1} of the intervals. We will do so in three steps.

1. *The images of* $[a, A)$ *and* $(A, d]$.

The image of $[a, A) = \{(x, y) | y = -\beta, -\beta \le x < s\}$ under T^{-1} is a curve of the form

$$x = \frac{6y(1-y) + \beta}{\alpha(s-y)}, \tag{19}$$

defined for $-\beta \le y < s$, thus, $s - y$ is positive here. Denote $N_1(y) \equiv 6y(1 - y) + \beta$. Suppose that the following inequality

$$N_1(s) \equiv 6s(1-s) + \beta > 0 \tag{20}$$

is valid (for example, it holds if $0 < s < 1$). Then, the curve $T^{-1}([a, A))$ has the following asymptotic behavior as $y \to s - 0$:

$$\text{for } \alpha > 0 : x \to +\infty \quad \text{as } y \to s - 0;$$
$$\text{for } \alpha < 0 : x \to -\infty \quad \text{as } y \to s - 0.$$

(see Figs. 12(b)–12(d) for $\alpha > 0$ and 14(b)–14(d) for $\alpha < 0$). Moreover, curve (19) is monotone in this case. Indeed,

$$\frac{\partial x}{\partial y} = \frac{6y^2 - 12sy + 6s + \beta}{\alpha(s-y)^2} \tag{21}$$

and the numerator $N_2 \equiv 6y^2 - 12sy + 6s + \beta$ has the discriminant $\Delta_2 \equiv 6(6s^2 - 6s - \beta)$ being negative when (20) holds.

The image of $(A, d] = \{(x, y) | y = -\beta, s < x \le 1 + \beta\}$ under T^{-1} is a curve of the form (19) again, defined only for $s < y \le 1 + \beta$. Thus, $(s - y)$ is negative in this case and if (20) holds, the curve is monotone and the following asymptotic takes place:

$$\text{for } \alpha > 0 : x \to -\infty \quad \text{as } y \to s + 0;$$
$$\text{for } \alpha < 0 : x \to +\infty \quad \text{as } y \to s + 0.$$

(see Figs. 12(b)–12(d) for $\alpha > 0$ and 14(b)–14(d) for $\alpha < 0$).

Suppose now that s is such that $N_1(s) = 6s(1-s)+\beta < 0$. This inequality implies that s is away from the interval (s_1, s_2), where

$$s_{1,2} = \frac{1}{2}\left(1 \pm \sqrt{1+\frac{2}{3}\beta}\right) \tag{22}$$

are the roots of the equation $N_1(s) = 0$. Note that $s_1 < 0, s_2 > 1$ and

$$s_1 = -\frac{1}{6}\beta + O(\beta^2), \quad s_2 = 1 + \frac{1}{6}\beta + O(\beta^2) \tag{23}$$

when β is small. If $s < s_1$ or $s > s_2$ the asymptotic behavior of curves $T^{-1}([a, A))$ and $T^{-1}((A, d])$ is cardinally changed:

$$T^{-1}([a, A)) : x \to -\infty \text{ (resp. } +\infty) \text{ as } y \to s-0$$
$$\text{for } \alpha > 0 \text{ (resp. for } \alpha < 0),$$
$$T^{-1}([d, A)) : x \to +\infty \text{ (resp. } -\infty) \text{ as } y \to s-0$$
$$\text{for } \alpha > 0 \text{ (resp. for } \alpha < 0)$$

(see Figs. 12(a) and 12(e) for $\alpha > 0$ and 14(a) and 14(e) for $\alpha < 0$). Moreover, both curves are not monotone here. Indeed, in this case the numerator $N_2 \equiv 6y^2 - 12sy + 6s + \beta$ from (21) can vanish since its discriminant $\Delta_2 \equiv 6(6s^2 - 6s - \beta)$ is positive. The corresponding extremum points are $y_1^* = s - \sqrt{q(s)}$ for the curve $T^{-1}([a, A))$ (since $y < s$ for it) and $y_2^* = s + \sqrt{q(s)}$ for the curve $T^{-1}([d, A))$ (since $y > s$ here), where $q(s) = s^2 - s - \beta/6 > 0$.

Consider the case $s < s_1$. Then the extremum point, say x_1^*, of the curve $T^{-1}([a, A))$ exists and equals

$$x_1^* = \frac{6(s-\sqrt{q})(1-s+\sqrt{q})+\beta}{\alpha\sqrt{q}}$$
$$= \frac{6}{\alpha}\left[\frac{s(1-s)+\dfrac{\beta}{6}}{\sqrt{q}} - 1 + 2s - \sqrt{q}\right].$$

Thus, sign $x_1^* = -\text{sign}(\alpha)$ and $|x_1^*| > 6|\alpha|^{-1}$ (all terms in $[\cdot]$ are negative). This implies that the curve $T^{-1}([a, A))$ is posed as whole outside Q_β. On the other hand, the curve $T^{-1}((A, d])$ intersects Q_β in a regular way. Indeed, $y = 1/2$ is in the domain of definition and, thus,

$$|x^*| \geq \frac{\dfrac{3}{2}+\beta}{|\alpha|\left(\dfrac{1}{2}+\beta\right)}$$

and sign $x_1^* = -\text{sign}\,\alpha$.

In the case when $s > s_2$, the situation becomes opposite: the curve $T^{-1}((A, d])$ is posed as whole outside Q_β, while the curve $T^{-1}([a, A))$ intersects Q_β in a regular way (the proof is quite similar). Note that the curves $T^{-1}([a, A))$ and $T^{-1}((A, d])$ always have the opposite asymptotic behavior at infinity.

2. *The image of* $[b, B)$ *and* $(B, c]$.

The image of $[b, B) = \{(x, y) : y = 1+\beta, -\beta \leq x < s\}$ under T^{-1} is a curve of the form

$$x = \frac{6y(1-y)-1-\beta}{\alpha(s-y)}, \tag{24}$$

defined for $-\beta \leq y < s$. Thus, $(s-y)$ is positive here. When $y = s$, the numerator N_3 in (24) equals $N_3 = 6s(1-s)-1-\beta$. Thus, $N_3(s) = 0$ at $s = s_{1,2}^*$, where

$$s_{1,2}^* = \frac{1}{2}\left(1 \pm \sqrt{\frac{1}{3}(1-2\beta)}\right). \tag{25}$$

Accordingly, $N_3(s)$ is positive for $s_1^* < s < s_2^*$. In this case, the curve $T^{-1}([b, B))$ behaves as follows:

$$\text{for } \alpha > 0 : x \to -\infty \quad \text{as } y \to s-0;$$
$$\text{for } \alpha < 0 : x \to +\infty \quad \text{as } y \to s-0.$$

(see Figs. 12(c) for $\alpha > 0$ and 14(c) for $\alpha < 0$). Besides, curve (24) is monotone in the case when $s \in (s_1^*, s_2^*)$. Indeed, we have

$$\frac{\partial x}{\partial y} = \frac{6y^2 - 12sy + 6s - 1 - \beta}{\alpha(s-y)^2}$$

and the discriminant D of the numerator, $D \equiv 6(6s^2 - 6s + 1 + \beta)$, is negative if $s_1^* < s < s_2^*$.

Consider now the case $s < s_1^*$. Then, $N_3(s) < 0$ and the asymptotic behavior of the curve $T^{-1}([b, B))$ is as follows:

$$\text{for } \alpha > 0 : x \to +\infty \quad \text{as } y \to s-0;$$
$$\text{for } \alpha < 0 : x \to -\infty \quad \text{as } y \to s-0.$$

(see Figs. 12(a)–12(e) for $\alpha > 0$ and 14(a)–14(e) for $\alpha < 0$). Moreover, curve (24) is not monotone in this case. Indeed, the equation $6y^2 - 12sy + 6s - 1 - \beta = 0$ has the solution

$$y* = s - \sqrt{s^2 - s + \frac{1+\beta}{6}}$$

(satisfying the condition $y < s$). In this case, the curve (24) has the extremum $x^* = x(y^*)$ with $N_3(y^*) < 0$ since $s < s_1^*$.

In the case $s > s_2^*$ we have again that $N_3(s)$ is negative and, thus, the asymptotic behavior of the curve $T^{-1}([b, B))$ is the same as in the previous case. Besides, curve (24) is not monotone again. However, the extremum $x^* = x(y^*)$ has another sign, since the function $N_3(y)$ may now have positive values. In particular, $y = 1/2$ belongs to the domain of definition of N_3, and $N_3(1/2) = (1/2) - \beta > 0$. Thus, using (24) we find that

$$|x^*| \geq \frac{\frac{1}{2} - \beta}{|\alpha| \left(\frac{1}{2} + \beta\right)}$$

and sign $x^* = \text{sign}\ \alpha$.

The case of the curve $T^{-1}((B, c])$, where $(B, c] = \{(x, y) : y = 1 + \beta, s < x \leq 1 + \beta\}$, is considered rather analogously. Here the curve $T^{-1}((B, c])$ satisfies again Eq. (24), defined now only for $s < y \leq 1 + \beta$. Thus, $s - y$ is negative. Then, if $s_1^* < s < s_2^*$, values of $N_3(s)$ are positive and, hence, the curve $T^{-1}((B, c])$ is monotone and behaves as follows (in the opposite way to $T^{-1}([b, B))$):

$$\begin{aligned} &\text{for } \alpha > 0 : x \to +\infty \quad \text{as } y \to s + 0; \\ &\text{for } \alpha < 0 : x \to -\infty \quad \text{as } y \to s + 0. \end{aligned}$$

(see Figs. 12(c) for $\alpha > 0$ and 14(c) for $\alpha < 0$). If $s > s_2^*$, the asymptotic behavior of the curve $T^{-1}((B, c])$ becomes as follows:

$$\begin{aligned} &\text{for } \alpha > 0 : x \to -\infty \quad \text{as } y \to s + 0; \\ &\text{for } \alpha < 0 : x \to +\infty \quad \text{as } y \to s + 0. \end{aligned}$$

(see Figs. 12(a)–12(e) for $\alpha > 0$ and 14(a)–14(e) for $\alpha < 0$). As in the previous case, the curve $T^{-1}((B, c])$ is not monotone. Indeed, the equation $6y^2 - 12sy + 6s - 1 - \beta = 0$ has the solution

$$y* = s + \sqrt{s^2 - s + \frac{1 + \beta}{6}}$$

(satisfying the condition $y > s$). In this case, the curve $T^{-1}((B, c])$ has a maximum $x^* = x(y^*)$ at which the value of $N_3(y^*)$ is negative since $s > s_2^*$.

In the case $s < s_1^*$ we have that $N_3(s)$ is negative again and, thus, the asymptotic behavior of the curve $T^{-1}((B, c])$ is the same as in the case $s > s_2^*$. Besides, curve $T^{-1}((B, c])$ is not monotone again. However, $N_3(y^*)$ is positive at the extremum point $x^* = x(y^*)$. As in the previous case, using the fact that $y = 1/2$ is from the domain of definition for $T^{-1}((B, c])$, we obtain the following estimate

$$|x^*| \geq \frac{\frac{1}{2} - \beta}{|\alpha| \left(\frac{1}{2} + \beta\right)}$$

and, besides, sign $x^* = -\text{sign}\ \alpha$, since in this case $(s - y)$ is always negative.

3. The images of the intervals of $[a, b]$ and $[c, d]$ under T^{-1} are horizontal segments of the lines $y = -\beta$ and $y = 1 + \beta$, respectively, whose endpoints are given by (18).

These reconstructions are closely related to the bifurcations which (without leading off the hyperbolicity) change drastically the behavior of stable and unstable manifolds of the periodic points and influence the horseshoes' geometry. We do not study these bifurcations in detail now (leaving it to the forthcoming paper); we just note that infinitely many instant bifurcations occur while transitioning from orientable to nonorientable Smale horseshoes (and vice versa).

Acknowledgments

The authors thank V. S. Afraimovich, V. Z. Grines and D. Turaev for fruitful discussions. S. Gonchenko is grateful to NSC (Taiwan) for the support during his visit. S. Gonchenko and M. Malkin were supported in part by RFBR grant Nos. 07-01-00566, 07-01-00715, 08-01-00083, 08-01-00547, and by MNTI-RFBR grant No. 06-01-72023. M.-C. Li was partially supported by NSC grant No. 95-2115-M-018-004.

References

Afraimovich, V. S., Bykov, V. V. & Shilnikov, L. P. [1977] "On the origin and structure of the Lorenz attractor," *Soviet Phys. Dokl.* **22**, 253–255.

Afraimovich, V. S., Bykov, V. V. & Shilnikov, L. P. [1983] "On structurally unstable attracting sets of Lorenz attractor type," *Trans. Moscow Math. Soc.* **44**, 153–216.

Afraimovich, V. S. [1984] "Strange attractors and quasiattractors," *Nonlinear and Turbulent Processes in Physics*, **3**, ed. Sagdeev, R. Z. (Gordon and Breach, Harwood Academic Publishers), pp. 1133–1138.

Afraimovich, V. & Hsu, S.-B. [2002] *Lecture on Chaotic Dynamical Systems*, AMS/IP, Studies in Advanced Mathematics, Vol. 28.

de Melo, W. & van Strien, S. [1993] *One-Dimensional Dynamics* (Springer-Verlag, NY).

Devaney, R. & Nitecki, Z. [1979] "Shift automorphisms in the Hénon mapping," *Comm. Math. Phys.* **67**, 137–146.

Gardini, L., Abraham, R., Record, R. J. & Fournier-Prunaret, D. [1994] "A double logistic map," *Int. J. Bifurcation and Chaos* **4**, 145–176.

Gavrilov, N. K. & Shilnikov, L. P. [1972] "On three-dimensional dynamical systems close to systems with a structurally unstable homoclinic curve, Part 1," *Math. USSR Sb.* **17**, 467–485.

Gavrilov, N. K. & Shilnikov, L. P. [1973] "On three-dimensional dynamical systems close to systems with a structurally unstable homoclinic curve, Part 2," *Math. USSR Sb.* **19**, 139–156.

Gonchenko, S. V., Shilnikov, L. P. & Turaev, D. V. [1993] "Dynamical phenomena in systems with structurally unstable Poincare homoclinic orbits," *Russian Acad. Sci. Dokl. Math.* **47**, 410–415.

Gonchenko, S. V., Shilnikov, L. P. & Turaev, D. V. [1996] "Dynamical phenomena in systems with structurally unstable Poincare homoclinic orbits," *Chaos* **6**, 15–31.

Gonchenko, S. V. & Gonchenko, V. S. [2000] "On Andronov–Hopf bifurcations of two-dimensional diffeomorphisms with homoclinic tangencies," Weierstrass Institute for Applied Analysis and Stochastics-Preprint No. 556, Berlin, <http://www.wias-berlin.de/main/publications/wias-publ/index.cgi.en>.

Gonchenko, S. V. & Gonchenko, V. S. [2004] "On bifurcations of birth of closed invariant curves in the case of two-dimensional diffeomorphisms with homoclinic tangencies," *Proc. Math. Steklov Inst.* **244**, 80–105.

Gonchenko, V. S., Kuznetsov, Yu. A. & Meijer, H. G. E. [2005a] "Generalized Henon map and bifurcations of homoclinic tangencies," *SIAM J. Appl. Dyn. Sys.* **4**, 407–436.

Gonchenko, S. V., Shilnikov, L. P. & Turaev, D. V. [2005b] "On the dynamical properties of diffeomorphisms with homoclinic tangencies," *J. Math. Sci. (N.Y.)* **126**, 1317–1343.

Grines, V. Z. [1975] "On topological conjugacy of diffeomorphisms of a two-manifold on one-dimensional basic sets. Part I," *Trans. Moscow Math. Soc.* **32**, 35–60.

Hénon, M. [1976] "A two-dimensional mapping with a strange attractor," *Comm. Math. Phys.* **50**, 69–77.

Juang, J., Li, M.-C. & Malkin, M. [2005] "Multidimensional perturbations of chaotic one-dimensional maps and their applications," Preprint of Institute of Mathematics, Academia Sinica, MIAS-2005, Taipei.

Li, M.-C. & Malkin, M. [2004] "Bounded nonwandering sets for polynomial mappings," *J. Dyn. Contr. Sys.* **10**, 377–389.

Li, M.-C. & Malkin, M. [2006] "Topological horseshoes for perturbations of singular difference equations," *Nonlinearity* **19**, 795–811.

Marotto, J. R. [1978] "Snap-back repeller imply chaos in $\mathbb{R}^n$," *J. Math. Anal. Appl.* **63**, 199–223.

Misiurewicz, M. & Zgliczynski, P. [2001] "Topological entropy for multidimensional perturbations of one-dimensional maps," *Int. J. Bifurcation and Chaos* **11**, 1443–1446.

Mira, C. [1987] *Chaotic Dynamics* (World Scientific, Singapore).

Mira, C., Gardini, L., Barugola, A. & Cathala, J.-C. [1996] *Chaotic Dynamics in Two-Dimensional Noninvertible Maps* (World Scientific, Singapore).

Palis, J. & Takens, F. [1993] *Hyperbolicity and Sensitive Chaotic Dynamics at Homoclinic Bifurcations* (Cambridge Univ. Press).

Robinson, C. [1999] *Dynamical Systems: Stability, Symbolic Dynamics and Chaos*, 2nd edition (CRC Press, Boca Raton).

Shilnikov, L. P., Shilnikov, A. L., Turaev, D. V. & Chua, L. O. [1998] *Methods of Qualitative Theory in Nonlinear Dynamics, Part I* (World Scientific, Singapore).

Shilnikov, L. P., Shilnikov, A. L., Turaev, D. V. & Chua, L. O. [2001] *Methods of Qualitative Theory in Nonlinear Dynamics, Part II* (World Scientific, Singapore).

Tedeschini-Lalli, L. & Yorke, J. A. [1986] "How often do simple dynamical processes have infinitely many coexisting sinks?" *Commun. Math. Phys.* **106**, 635–657.